Review and Comparison of Control Strategies in Active Power Decoupling

Yonglu Liu, *Member, IEEE*, Wanlu Zhang, Yao Sun, *Member, IEEE*, Mei Su, *Member, IEEE*, Guo Xu, *Member, IEEE*, and Hanbing Dan, *Member, IEEE*

***Abstract*—The active power-decoupling (APD) method is an effective solution to handle the inherent double-line frequency ripple power in single-phase power systems. It removes the bulky passive devices and facilitates the improvement of the system power density and even the reliability. This article provides a comprehensive review of the prior-art and state-of-the-art control strategies in APD. They are categorized into four groups according to the basic control ideas of "power balance," "harmonic suppression," "volt-second balance/charge balance," and "virtual impedance." And the specific control strategies under each control idea are discussed and compared. The pros and cons of each control idea are also presented. Finally, this article draws a sketch of the global trends in APD control.**

***Index Terms*—Active power decoupling (APD), control strategies, double-line frequency ripple power, single-phase systems.**

Nomenclature

ANFIS	Adaptive network-based fuzzy inference system.
APD	Active power decoupling.
APFC	Active power filter-based control.
BPF	Bandpass filter.
CBBC	Charge balance-based control.
CCCS	Current-controlled current source.
CCM	Continuous conduction mode.
DCM	Discontinuous conduction mode.
DVRC	Dynamic voltage restorer-based control.
HPF	High-pass filter.
HSBC	Harmonic suppression-based control.
LED	Light-emitting diode.
LPF	Low-pass filter.
NF	Neural filter.
P	Proportional (controller).
PBBC	Power balance-based control.
PFC	Power factor correction.
PI	Proportional–integral (controller).
PID	Proportional–integral derivative (controller).
PR	Proportional–resonant (controller).
P&O	Perturb and observe (controller).
PV	Photovoltaic.
qZSIs	Quasi-*Z*-source inverters.
RF	Resonant filter.
SMC	Sliding-mode controller.
TSMC	Total sliding-mode controller.
VBBC	Volt-second balance-based control.
VCVS	Voltage-controlled voltage source.
VIBC	Virtual-impedance-based control.
VSC	Voltage-source converter.
ZSIs	*Z*-source inverters.

Manuscript received December 22, 2020; revised April 13, 2021; accepted May 28, 2021. Date of publication June 8, 2021; date of current version August 16, 2021. This work was supported in part by the National Natural Science Foundation of China under Grant 61903381, in part by Changsha City Science and Technology Plan Project under Grant kq2009007, in part by the Hunan Provincial Key Laboratory of Power Electronics Equipment and Grid under Grant 2018TP1001, and in part by the Fundamental Research Funds in the Central South University under Grant 2021zzts0704. Recommended for publication by Associate Editor M. S. ElMoursi. *(Corresponding author: Guo Xu.)*

The authors are with the School of Automation, Central South University, Changsha 410083, China, and also with Hunan Provincial Key Laboratory of Power Electronics Equipment and Grid, Central South University, Changsha 410083, China. (e-mail: liuyonglu@csu.edu.cn; zhang_wanlu@csu.edu.cn; yaosuncsu@gmail.com; sumeicsu@csu.edu.cn; xuguocsu@csu.edu.cn; daniel698@sina.cn).

Color versions of one or more figures in this article are available at https://doi.org/10.1109/TPEL.2021.3087170.

Digital Object Identifier 10.1109/TPEL.2021.3087170

I. Introduction

SINGLE-PHASE power electronics interface is widely used in various occasions, such as photovoltaic (PV) power generation [1], light-emitting diode (LED) lighting driving [2], and electric vehicle charging [3]. It is well known that the instantaneous power at the ac side fluctuates at twice the grid frequency (including a second-order ripple power). And the dc-side power can be constant (connected by a PV panel, for instance) or timing varying (connected by a nonlinear load, for instance) [1]. Then, there exists a power mismatch between the ac side and the dc side.

The active power-decoupling (APD) method is an effective solution to handle the power mismatch and then promotes the increment of system power density [4]. Its principle is to divert the mismatched power to a small capacitor (film or ceramic capacitors) and store it by swinging its voltage, as shown in Fig. 1. In the little box challenge competition (inciting innovations and developments for high-power-density single-phase inverters) sponsored by Google and the IEEE Power Electronics Society in 2014, nearly all the participating teams adopted the APD technique to deal with the double-line frequency ripple power and increase the power density [5].

APD has attracted much attention in recent years and has been studied in various applications. The main research includes the various decoupling circuit topologies and their control

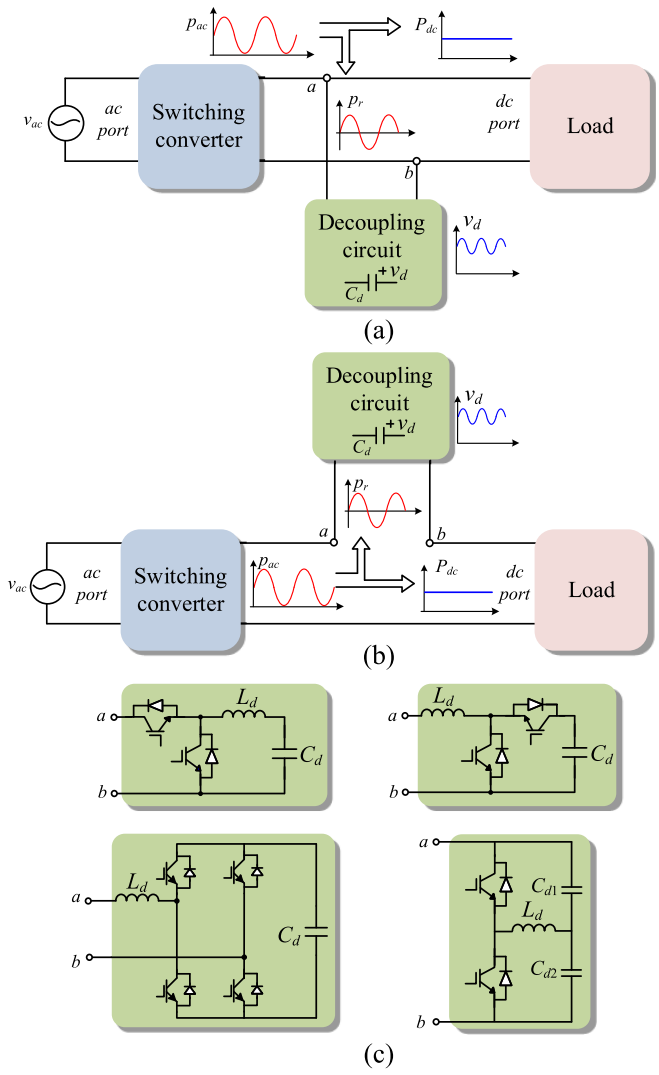

Fig. 1. Decoupling circuit configuration with two ports. (a) Parallel structure. (b) Series structure. (c) Commonly used decoupling circuits.

strategies. For the topologies, from the view of whether the component-multiplexing exists, the decoupling circuit topologies are divided into independent and dependent ones [4]. In the former, the decoupling operates independently with the original converter and, in the latter, the power semiconductor devices or capacitors are shared with the original converter partially and even completely. In another review article [6], the decoupling topologies are divided into rectifiers, inverters, and bidirectionals. And a second broad classification has been done according to whether the topology has galvanic isolation or not. For the specific applications, in the review literature [7], the decoupling topologies developed for PV system are categorized into PV-side decoupling, dc-link decoupling, and ac-side decoupling in terms of the decoupling capacitor locations. In [8], the decoupling circuits applied for current-source converters are summarized and compared. In [9], the power-decoupling strategies of single-phase ZSIs/qZSIs were discussed and compared in terms of their passive components' sizes, control methods, and ripple attenuation performances. In [10], the application of different APD circuits and decoupling control strategies (called the active compensation approach) in the fuel cell system is discussed. The literature [11] presented a benchmark of the ac and dc APD circuits for kilowatt scale single-phase inverters. And the boost-type dc power-decoupling circuit is found to be best suited for this specific application. To achieve excellent decoupling performance, the controller design is crucial. The identification of effective control for APD has attracted increasing research interests in both academia and industry. And a large number of control schemes have been developed [12]–[108], [112]–[115]. However, no comprehensive investigation has been carried out to reveal basic control ideas, main features, and suitable applications of these control strategies. This is the gap this article will fill.

This article aims at providing an overview of prior-art and state-of-the-art decoupling control methods in APD. According to the control ideas, the decoupling control methods are classified into four kinds: power balance-based control (PBBC) [12]–[38], harmonic suppression-based control (HSBC) [39]–[78], volt-second balance-based/ charge balance-based control (VBBC/CBBC) [79]–[108], and virtual-impedance-based control (VIBC) [112]–[115]. Besides, for each control idea, there are also a number of specific control strategies, whose detailed explanations, comparisons, and discussions are summarized. The classification and analyses of control ideas and their specific strategies will support researchers and developers to select the most suitable control strategy depending on the specific application.

The rest of this article is organized as follows. Sections II, III, IV, and V introduce the basic control ideas and controller schemes of PBBC, HSBC, VBBC/CBBC, and VIBC, respectively. Section VI presents the experimental case study. Finally, Section VII discusses the four methods and draws the conclusion in this article.

II. PBBC Method

A. Control Idea

Suppose the ripple power is fully buffered by the decoupling capacitor or inductor. Then, according to the power balance, the decoupling capacitor voltage or the decoupling inductor current can be obtained and taken as a control target. Once the referenced voltage or current is well tracked, the ripple power is thought to be well handled. Taking the single-phase rectifier as an example, Fig. 2 shows the specific control process.

The precise voltage/current reference is critical to decoupling performance. Besides, it is also a challenge for the controller design to track the reference voltage/current rapidly and accurately when the voltage/current contains a large number of harmonics. These two issues have drawn the attention of many researchers.

B. Decoupling Voltage/Current Reference

The voltage/current reference can be obtained by the methods of open-loop or closed-loop calculation. The open-loop calculation process is briefly introduced as follows.

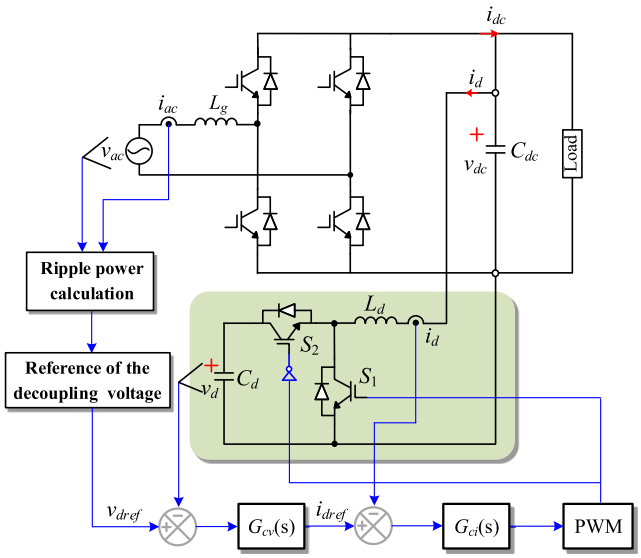

Fig. 2. Control scheme for PBBC method.

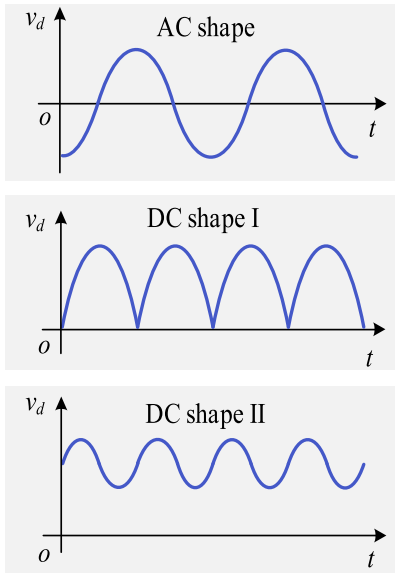

Fig. 3. Decoupling capacitor voltage reference for PBBC method.

Suppose the grid voltage and current are

$$v_{\rm ac} = V\cos(\omega t), \quad i_{\rm ac} = I\cos(\omega t + \varphi) \tag{1}$$

where V and I are the amplitudes of the grid voltage and current, respectively, ω is the grid frequency, and φ is the displacement angle. Then, the instantaneous power $p_{\rm ac}$ of the grid is expressed as

$$p_{\rm ac} = v_{\rm ac} i_{\rm ac} = \underbrace{VI\cos(\varphi)/2}_{P_{\rm dc}} + \underbrace{VI\cos(2\omega t + \varphi)/2}_{p_r} \tag{2}$$

which includes a constant power $P_{\rm dc}$ and a 2ω ripple power p_r. Considering the case of rectification and p_r is absorbed by the decoupling capacitor C_d, we can obtain the following equation:

$$\frac{1}{2}C_d\frac{dv_d^2}{dt} = VI\cos(2\omega t + \varphi)/2. \tag{3}$$

By solving (3), the decoupling capacitor voltage $v_d(t)$ meets

$$v_d^2(t) = \frac{VI\sin(2\omega t + \varphi)}{2\omega C_d} + K \tag{4}$$

where K is a constant that affects the voltage waveforms. After some elementary calculations, the decoupling capacitor voltage can be expressed as

$$v_d(t) = \begin{cases} V_d\sin(\omega t + \theta), & K = \frac{VI}{2\omega C_d}, \text{ AC shape} \\ V_d|\sin(\omega t + \theta)|, & K = \frac{VI}{2\omega C_d}, \text{ DC shape I} \\ \sqrt{A\sin(2\omega t + \varphi) + K}, & K > \frac{VI}{2\omega C_d}, \text{ DC shape II} \end{cases} \tag{5}$$

where

$$V_d = \sqrt{\frac{VI}{\omega C_d}}, \quad \theta = \frac{\varphi}{2} + \frac{\pi}{4}, \text{ and } A = \frac{VI}{2\omega C_d}.$$

From (5), the decoupling capacitor voltage can be controlled to be ac shape or dc shape, as depicted in Fig. 3. When the inductor is used as the storage element, its current waveform can be analyzed similarly [12], [13].

For many developed control methods for decoupling applications [14]–[25], the voltage v_d in (5) is directly used as the control reference. However, the open-loop calculation method has the following disadvantages.

1) Sensitive to the parameter disturbances since v_d depends on the precise knowledge of output power (VI/2), the value of the decoupling capacitor (C_d), the grid frequency (ω), and phase difference (φ).
2) Inaccurate calculation due to ignoring the power losses caused by the active switches and passive components.
3) Hard to handle the situations where the instantaneous power mismatch is not purely sinusoidal, for example, the load is nonlinear or the grid includes background harmonics.

To improve the precision of the decoupling voltage, in [26] and [27], the real-time load power (VI/2) is computed and substituted into (5). In [28], the grid current amplitude I and the phase angle φ are obtained according to the detected grid current by using a notch filter and a 90° phase shifter. For dealing with the case of the nonlinear load, in [29], the ripple power is estimated and replace the right side of (3) to determine the voltage reference. In [30], the phase information of the ac decoupling capacitor voltage is extracted from the dc bus voltage ripple by adopting single-input space vector theory.

Once the ripple power is not absorbed by C_d, the dc bus voltage will oscillate. Therefore, the voltage error between the dc bus voltage reference and its practice value can be taken as an indicator to reflect the decoupling performance. In [31]–[33], the voltage error is used to modify the amplitude V_d and the angle θ. However, some approximations have been made during extracting the ripple power from the dc bus voltage. In [34], the voltage error is fed back to modify the amplitude A. These methods achieve better decoupling performance at the cost of complexity control. However, both of them fail to work when the grid voltage or current is not purely sinusoidal or the load is nonlinear.

In the aforementioned works, the voltage or current reference is obtained from the view of the average value over a switching cycle. To improve the decoupling performance, the pulse energy modulation [35]–[37] has been developed. The demanded energy provided by the decoupling capacitors is obtained by integrating the power over a switching period. This control removes the second-order harmonic in the dc current without introducing the low-order harmonic components. To improve the dynamic performance, the direct instantaneous ripple power predictive control [38] is proposed. The control output voltage is determined by minimizing the cost function, which is defined as

$$f_{\text{cost}}(k) = |p_{\text{ripple}}(k) - p_c(k+1)| \tag{6}$$

where $p_{\text{ripple}}(k)$ is the ripple power at the kth time instant and $p_c(k+1)$ is the power provided by the decoupling capacitor during the $(k+1)$th switching period. Note that the voltage reference in [38] is the control output voltage rather than the decoupling capacitor voltage and the control is still an open loop.

C. Controller Schemes

For the controller, when v_d is controlled to be an ac waveform, the periodic controller, such as proportional–resonant (PR) controller [13], [23], [30]–[33], is a good choice according to the internal model principle. In [13], an adaptive network-based fuzzy inference system (ANFIS) is developed and performs better transient performance compared with the PR controller. In [23], an extra zero-sequence voltage derived from the three-phase-leg SPWM voltages is injected to reduce the decoupling capacitance.

When v_d is controlled to be a dc waveform, there exist two scenarios. For dc shape I, the reference voltage is a full-wave rectified sine wave and contains rich harmonics. The sharp turns at the bottom of the voltage waveform indicate rich harmonics, which are difficult to track. The reported control includes multiresonant control [12] and band current control [24]. For dc shape II, a large dc offset is usually designed and the developed control includes proportional (P) control [14], proportional–integral (PI) control [19], [21], [26], [27], [29], bang–bang control [18], type III compensator [20], and model predictive control [22], [38].

D. Summary

PBBC strategies are summarized in Table I. This control concept is easy to understand and implement. And the control scheme is independent of the original rectifier/inverter control and universal. However, the decoupling control is carried out indirectly. The precise voltage/current reference is difficult to obtain due to parameter drifts and power losses. Although the decoupling performance can be indicated by the error between the dc bus voltage reference and its practical value (a larger error indicates a worse decoupling performance), the challenge is how to modify the amplitude (V_d or A) and the phase shift (θ or φ) in a coordinated fashion (in Section III, some artificial intelligence approach will be introduced). Besides, this control method may be not suitable for nonlinear loads or the case with harmonics in the grid voltage in which the voltage/current reference is hard to calculate.

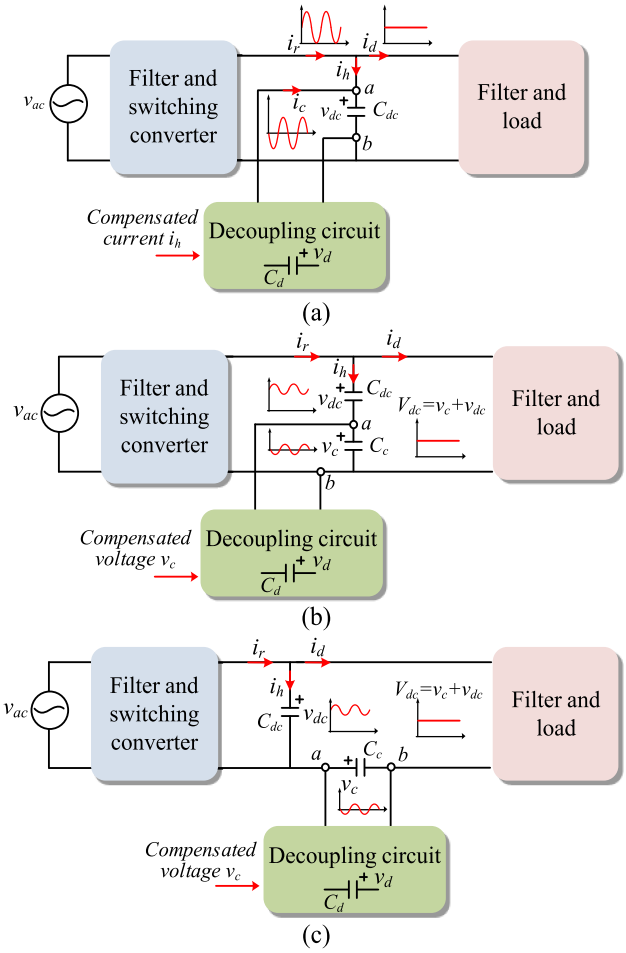

Fig. 4. Control schemes for the proposed HSBC method. (a) APFC. (b) DVRC I. (c) DVRC II.

III. HSBC Method

A. Control Idea

Suppose the dc bus voltage is constant. According to (2) and power balance, the rectified output current of the ac side is

$$i_r = \frac{p_{\text{ac}}}{V_{\text{dc}}} = \underbrace{VI\cos(\varphi)/(2V_{\text{dc}})}_{I_d} + \underbrace{VI\cos(2\omega t+\varphi)/(2V_{\text{dc}})}_{i_h} \tag{7}$$

where V_{dc} is the desired stiff bus voltage, I_d is the dc component current or the load current, and i_h is the second harmonic current. To maintain constant V_{dc}, there are two ways. One is to control the decoupling circuit to generate a counteraction current i_c (be the same amplitude but out of phase with the ripple current i_h) to offset i_h, as shown in Fig. 4(a). Therefore, the dc capacitor will be free of the low-frequency harmonic current. In this way, the decoupling circuit acts as a classical active power filter (APF) and it is called APF-based control (APFC) in this article. The other is to control the decoupling circuit to generate a compensated voltage v_c to offset the second ripple voltage in

TABLE I
SUMMARY OF PBBC METHODS

Reference	Decoupling circuit	Close loop calculation?	AC or DC reference	Controller	Close loop decoupling ?	Linear or nonlinear load	THD	DC link voltage /current ripple (peak-to-peak value)	Efficiency
[12]	Asymmetric H-bridge (multiplexing switches)	No	DC	Multi-resonant control	No	Linear	-	6V	-
[13]	H-bridge (multiplexing switches)	No	AC	PR and ANFIS	No	Linear	3.82%(PR)/ 4.02%(ANFIS)	10V(PR)/ 18V(ANFIS)	-
[14]	Asymmetric H-bridge	No	DC	P	No	Linear	7.2%	0.8A	84%
[15]/[16]	Boost/H-bridge	No	DC	PI	No	Linear	1.9%/-	50V /476mA	95.4%/-
[17]	H-bridge (multiplexing switches)	No	DC	PI	No	Linear	-	0.24A	-
[18]	Differential circuit	No	DC	Bang-bang control	No	Linear	-	0.05A	84.3%
[19]	Boost-type differential inverter	No	DC	PI	No	Linear	2.36%	-	83%
[21]	Buck (multiplexing switches)	No	DC	PI	No	Linear	4.1%	<0.6A	93.2%
[22]	Boost	No	DC	Model predictive control	No	Linear	-	1.18A	-
[23]	Buck	No	AC	PR	No	Linear	-	2.5V	91.5%
[24]	H-bridge	No	DC	Band current control	No	Linear	-	-	-
[25]	H-bridge (multiplexing switches)	No	AC	PI	No	Linear	-	30V	-
[26]/[27]	H-bridge	Yes	DC	PI	No	Linear	1.91% /4.24%	12V /8.87%	96.4% /94.9%
[28]	H-bridge (multiplexing switches)	Yes	AC	-	No	Linear	-	0.4A	98%
[29]	Buck	Yes	DC	PI	No	Nonlinear	-	4.2A	-
[30]	H-bridge (multiplexing switches)	Yes	AC	PR	Yes	Linear	<5%	20V	-
[31]-[33]	H-bridge (multiplexing switches)	Yes	AC	PR	Yes	Linear	-	14.2V/5V/5V	-/94.2%/-
[34]	Buck (multiplexing switches)	Yes	AC	-	Yes	Linear	3.556%	20V	90.72%
[35]	Differential buck-boost (multiplexing switches)	Yes	DC	-	No	Linear	5.9%	0.36A	88%
[36]	H-bridge	Yes	DC	-	No	Linear	<3.3%	<2V	91.4%
[37]	Buck	No	DC	-	No	Linear	5.5%	2A	92.8%
[38]	Buck	No	DC	Predictive control	No	Linear	-	10V	-

$v_{\rm dc}$, as shown in Fig. 4(b) and (c). Then, the sum of $v_{\rm dc}$ and v_c is still constant and equal to $V_{\rm dc}$. In this way, the decoupling circuit acts as a dynamic voltage restorer (DVR) and it is called DVR-based control (DVRC) in this article. Note that employing APFC or DVRC depends on the circuit structure. These two control strategies are most frequently used in the field of APD.

B. Compensated Voltage/Current Reference

To achieve excellent decoupling performance, the precise knowledge of the compensated current or voltage (i_c or v_c) is required. For APFC, the decoupling circuits are usually bidirectional boost, buck, buck–boost, and H-bridge circuits. The approach of obtaining the compensated current is universal.

Taking the boost circuit, as shown in Fig. 5, as an example, the block $G_{fi}(s)$ is used to extract the ripple current and its possible implements (some implements developed in other decoupling circuits are also illustrated here) are shown in Fig. 6. A simple method to obtain the compensated ripple current is to calculate it out directly. In [39], the second part in the right hand of (7) is used as the current command $i_{h\rm ref}$. In [40], the decoupling capacitor voltage is first emulated and then $i_{h\rm ref}$ is expressed as $C_d\frac{dv_d}{dt}$. In [41] and [42], by knowing i_r and $i_{\rm dc}$, $i_{h\rm ref}$ is calculated by $(i_r - i_{\rm dc})$. Another method is to extract from the rectified output current i_r by using filters. The usually used filters include the resonant filter (RF) [43]–[47], bandpass filter (BPF) [48]–[50], high-pass filter (HPF) [44], [45], [51]–[53], low-pass filter (LPF) [54], and neural filter (NF) [55]. The frequency of RF and BPF

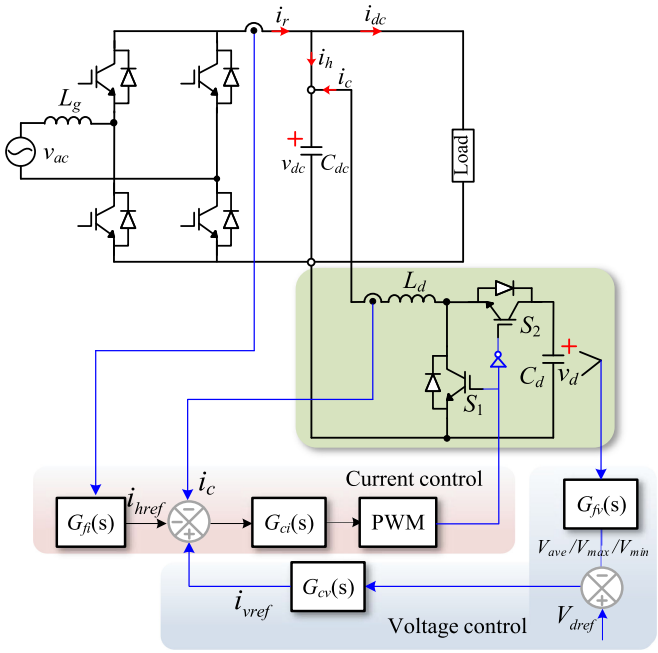

Fig. 5. Applying the HSBC method for boost decoupling circuit.

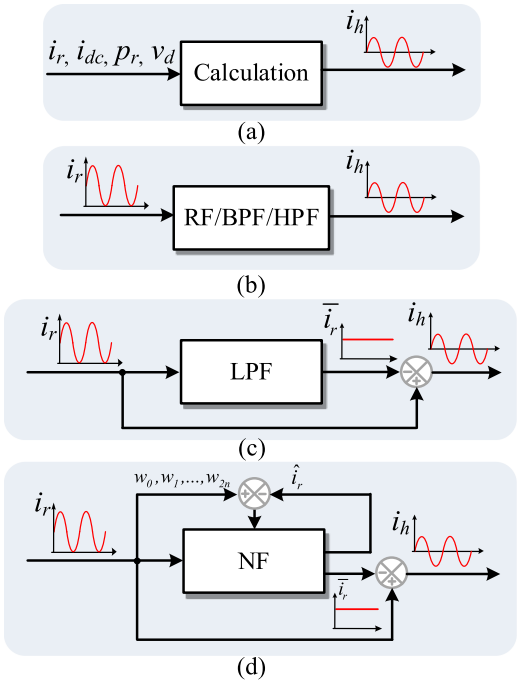

Fig. 6. Ripple current extraction methods and implements. (a) Direct calculation. (b) Direct extraction. (c) Indirect extraction. (d) Using NF.

is tuned at 2ω. And multi-RF and multi-BPF are needed when the load is nonlinear because other harmonic currents exist in i_r besides the second component. Unfortunately, although the usual used LPF and HPF are easy to implement, the response speed is limited. To achieve satisfactory filtering effectiveness and response speed, in [55], an adaptive linear neural network is taken as an NF to emulate the current i_r and its average value. The emulated value $\widehat{i_r}$ is fed back to modify the weighting

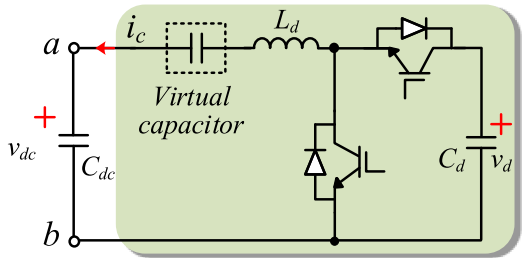

Fig. 7. Ripple current extraction method using a virtual capacitor.

coefficients. However, the NF is complex to accomplish. In [56], i_r is directly used as the ripple current reference straightway. By inserting a cascaded virtual capacitor, as shown in Fig. 7, the dc component of the current i_r is restrained and only the second harmonic current flows into the dc bus. The principle is similar to that of the HPF. And this is realized by introducing an integrator into the control loop.

For DVRC, the ac voltage in $v_{\rm dc}$ (v_r) can be acquired similarly and a voltage counteracting v_c (i.e., $v_c = -v_r$) is generated by the decoupling circuit. In addition, in [57] and [58], a low-frequency ripple sensor is used to obtain the ripple voltage. In [59] and [60], the ac component is extracted by subtracting the dc component from $v_{\rm dc}$.

C. Controller Schemes

For the decoupling circuit, two control loops are needed. One is the compensated current/voltage control loop to maintain a stiff dc bus voltage. And the current/voltage controller should be designed elaborately, especially when the load is nonlinear or the grid contains background harmonics (under this case, the compensated current or voltage includes other harmonics besides the second component). The other is a voltage control loop to prevent the overcharging and discharging of the decoupling capacitor v_d. The controllers are designed according to the characteristics of the decoupling circuits.

For the boost decoupling circuit (an example is shown in Fig. 5), the compensated current i_c is the inductor current. The inductor current is usually controlled to be continuous. In [51], $G_{ci}(s)$ is a simple PI controller, which is realized on the analog circuit, to track the compensated current. The output of the PI controller is taken as the modulation signal and compares with a sawtooth waveform to generate switching-driven signals. This is realized by supposing that the decoupling capacitor voltage contains only the dc component and the second harmonic component and ignoring other harmonic components. Therefore, the ripple power cannot be fully absorbed. Then, a feedforward control scheme [44], [45] is proposed to obtain the desired modulation signal, which contains the corresponding harmonic components. Obviously, the PI controller cannot achieve current tracking without error since the compensated current contains periodic components. In [43], a repetitive controller containing a positive feedback component is used to produce a compensation signal to adjust the current reference. Thus, the decoupling circuit can compensate the second harmonic current without

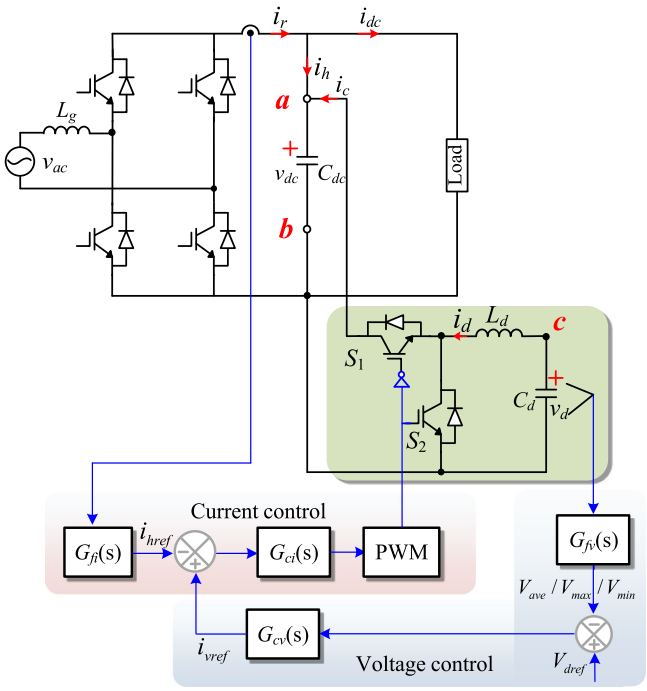

Fig. 8. Applying the HSBC method for buck decoupling circuit.

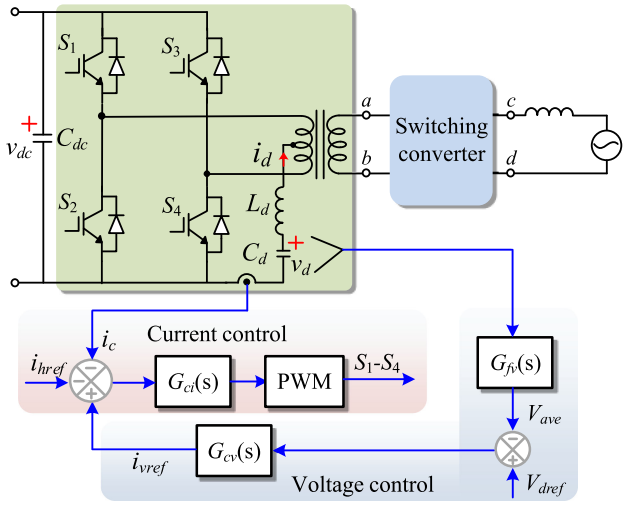

Fig. 9. Applying the HSBC method for multiplex decoupling circuit.

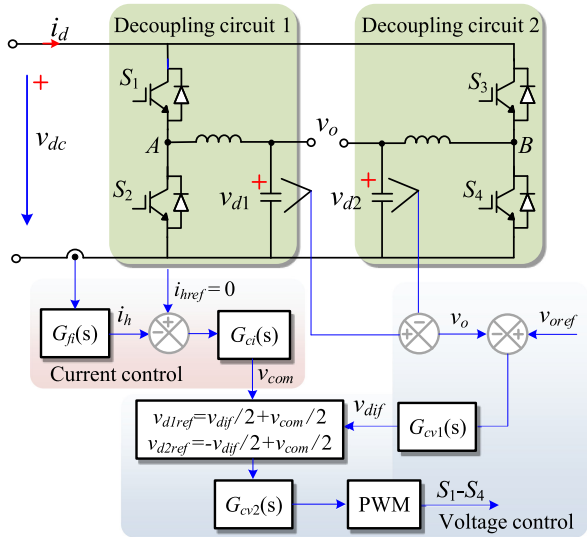

Fig. 10. Applying the HSBC method for buck differential inverter.

error. However, the repetitive control may lead to poor dynamic performance.

For the buck decoupling circuit (an example is shown in Fig. 8), the compensated current i_c is discontinuous. It seems that a discontinuous current control for the inductor L_d is popular [41], [42], [61], [62]. This is because the control is simple as a result of a single-loop control, the inductor current sensor is saved, and the dynamic response can be improved since the right half-plane zero is eliminated when the energy is transferred from C_d to $C_{\rm dc}$ (the decoupling circuit is actually a boost converter under this case). For some multiplex decoupling circuits in which the decoupling circuit shares switches with the rectifier (an example is shown in Fig. 9), the compensated current is just the inductor current, which is the same as the case of using a boost decoupling circuit. And the inductor current is controlled to be continuous by using PI [39], [40] or *RC* [49] controllers. In [48], to exactly follow the current reference within one switching cycle without being affected by the tolerance or parameter deviations of the passive components, a hybrid one-cycle control (OCC) is proposed and an excellent compensation performance is achieved.

For the buck–boost decoupling circuit [46], such as the buck decoupling circuit, the inductor is not directly connected to the dc bus and a discontinuous current control is also adopted. And for the H-bridge decoupling circuit [55], [57]–[60], [63]–[69], such as boost decoupling circuit, the inductor is directly connected to the dc and a continuous current control is usually adopted. In [55], a total sliding-mode controller (TSMC) is also designed to manipulate the decoupling circuit for injecting a suitable compensation current. For DVRC, the extracted ripple voltage is usually taken as the modulation signal and only a single voltage loop is used [57]–[60], [66], [67].

For the differential inverters [47], [50], [52], [53], [63], [70], [71] (an example is demonstrated in Fig. 10), the ripple current is provided by two decoupling circuits and the ripple power is buffered by swinging the common voltage $v_{\rm com}$ in v_{d1} and v_{d2}. The differential voltage $v_{\rm dif} = (v_{d1}\text{-}v_{d2})$ is a sinusoidal output voltage or the grid voltage. To realize the autonomous reference generation, the dc current ripple i_h is used to serve as the control variable. And the current controller $G_{ci}(s)$ is usually a multiresonant controller [52], [53], [70] because i_h may contain other harmonics, especially with nonlinear loads [53]. In [71], no filter is used to obtain the compensated current and a "perturb and observe" (P&O) method is used to adjust the amplitude and phase angle of the common voltage to minimize the second harmonic ripple current amplitude.

The dc-split decoupling circuits, as shown in Fig. 11, can be obtained by moving the electrical point from *b* to *c* in the buck

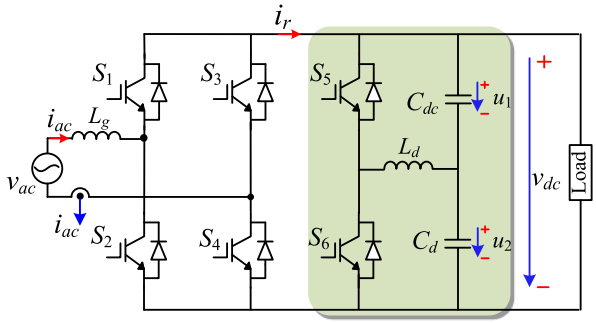

Fig. 11. Applying the HSBC method for the dc-split decoupling circuit.

decoupling circuit in Fig. 8. Both two capacitors $C_{\rm dc}$ and C_d are used to buffer the ripple power and also act as the dc output filter. For this topology structure, the HSBC is also suitable. The dc bus voltage is regulated by controlling the inductor current i_d. And the PR or SMC control techniques can be used [72]–[78].

In ideal cases, the decoupling circuit only handles reactive power (ripple power) and consumes no power. However, due to the power losses caused by the active and passive components, an additional voltage control loop is needed to stabilize the decoupling capacitor voltage, as shown in Figs. 5 and 8. This can be achieved via controlling the average voltage, the minimum voltage, the ripple ratio, or the maximum voltage of the decoupling capacitor at a given value, as summarized in Table II. Then, usually, a PI controller ($G_{cv}(s)$) will be employed to handle the voltage error and output an extra current term into the current reference. It should be noted that, for the differential inverters, the decoupling capacitor voltages are controlled to track their references rather than their average/minimum/maximum value. This is because the differential voltage v_o should be controlled to be a desired sinusoidal wave.

D. Summary

HSBC strategies are summarized in Table II. This control concept is widely adopted in the APD field. Many control strategies developed for APF applications can be used with minor modifications. And this control scheme is independent of the original rectifier/inverter control. However, this control method is an intrusive approach since the rectified current i_r should be sensed to extract the compensated ripple current (for the case of APFC) or a capacitor has to be inserted into the dc bus to provide a compensated voltage (for the case of DVRC). In addition, the accurate current/voltage reference during input/output power transient scenarios is almost impossible to obtain. This is because a dc component is also required in the compensated voltage/current during the transient. Besides, because of the phase delays of the filters, it takes some time for the compensated voltage/current to enter its steady-state value. When applying for rectifier (such as the cases, as shown in Figs. 5 and 8), this control method is usually open loop because the decoupling effect whether the dc bus voltage contains residual low-frequency components is not fed back. In addition, the frequency/frequencies of the compensated ripple reference must be known to design the PR or repetitive controller.

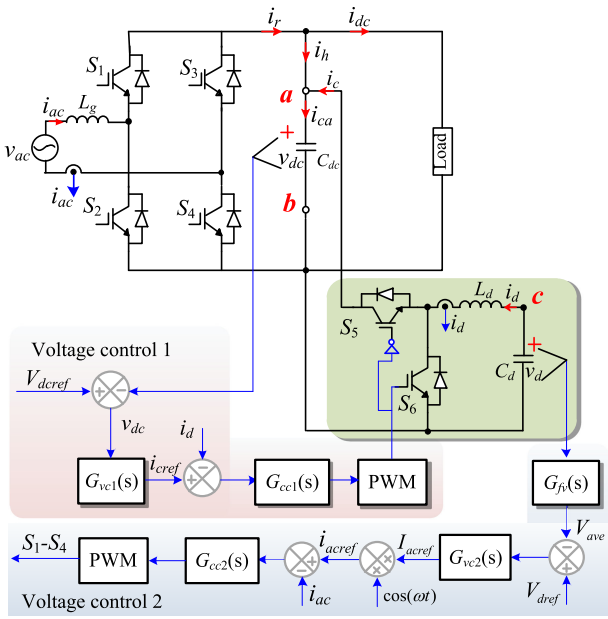

Fig. 12. Applying the CBBC method for buck decoupling circuit.

IV. VBBC/CBBC Method

A. Control Idea

For the dc side, the object of employing a decoupling circuit is to maintain a stiff bus voltage (bus current) for a voltage-source converter (current-source converter). From the view of the charge balance of a capacitor (volt-second balance of an inductor), the decoupling circuit keeps the charge balance of the dc bus filter capacitor (volt-second balance of the dc bus filter inductor) [79]–[88]. In this control method, the decoupling capacitor voltage reference is not required and no filter is needed to obtain the ripple voltage or current information. Since the dc bus capacitor voltage is directly controlled by the decoupling circuit, this control is also named direct voltage control [89], [90]. Besides, for no dedicated ripple power-decoupling controller is needed, this control is also called automatic-power-decoupling control [91], [92]. Based on this control concept, many control strategies have been developed [89]–[108].

B. Controller Schemes

To accomplish control aims, two voltage control loops are needed. Taking the buck decoupling circuit in Fig. 12 as an example, one voltage control is to regulate the dc bus capacitor voltage tightly. This control loop needs a high control bandwidth to achieve a fast regulation. The other is to maintain the decoupling capacitor voltage at a given voltage level $V_{\rm dref}$.

This control loop is designed to own a low bandwidth to avoid distorting the ac current. It can be found that this control concept should coordinate the decoupling control and rectification control. While, in the above-mentioned PBBC or HSBC, the decoupling control and the rectification control are independent.

Since the decoupling capacitor is charged and discharged alternately, the transfer function of the plant changes. And it is even unstable when the power flows back the dc bus (in this

TABLE II
SUMMARY OF HSBC METHODS

Reference	APFC or DVRC?	Decoupling circuit	Access to compensated current/voltage	Controller for compensated current/voltage	Close loop decoupling ?	Linear or nonlinear load	Decoupling voltage/current control	THD	DC link voltage /current ripple (peak-to-peak value)	Efficiency
[39]/[40]	APFC (multiplexing switches)	Buck	Calculation	PI	No	Linear	Average voltage control	<5% /<3%	2A /1.3A	90.5% /-
[41]	APFC	Buck	Calculation	Discontinuous current control	No	Pulse Load	Peak voltage control	-	4.5V	96%
[42]	APFC	Buck	Calculation	Discontinuous current control	Yes	Linear	Average voltage control	-	30.7mA	85.1%
[43]	APFC	Boost	RF	Repetitive control	No	Linear	Average voltage control	-	3V	-
[44]/[45]	APFC	Boost	HPF	PI+feed-forward	No	Linear	Average voltage control	-	56mA /0.57V	87% /89.5%
[46]	APFC	Buck-boost	RF	Discontinuous current control	No	Linear	Average /Minimum voltage control/Ripple ratio control	-	9V	-
[47]	APFC	Differential circuit	RF (2,4)	P	Yes	Linear	Waveform tracking	1.91%	-	96%
[48]	APFC	Buck	BPF	One-cycle control	No	Linear	Average voltage control	-	-	94%
[49]	APFC (multiplexing switches)	Buck Beijing converter	BPF	Repetitive controller	No	Linear	Minimum voltage control	3.2%	5V	91.5%
[50]	APFC	Differential circuit	BPF	P	Yes	Linear	Waveform tracking	-	0.1A	-
[51]	APFC	Boost	HPF	PI	No	Linear	Average voltage control	-	0.06A	87%
[52]	APFC	Differential circuit	HPF	Multi-resonant（1,2,3,4….）	Yes	Nonlinear	Waveform tracking	<2%	5A	-
[53]	APFC	Differential circuit	HPF	Multi-resonant（1,2,3,4….）	Yes	Linear	Waveform tracking	<1%	-	-
[54]	APFC	Boost	LPF	PI	No	Linear	Average voltage control	-	1.5A	-
[55]	APFC	H-bridge	NF	TMSC	No	Linear	-	-	0.5A	-
[56]	APFC	Boost	Virtual capacitor method	-	No	Linear	-	-	0.19A	-
[57]/[58]	DVRC	H-bridge	Low frequency ripple sensor	-	No	Linear	Waveform tracking	17.1% /-	20mA /100mV	86% /88.5%
[59]/[60]	DVRC	H-bridge	-	-	No	Linear	Average voltage control	-	10.8V /14.9V	-
[61]/[62]	APFC	Buck	Calculation	Discontinuous current control	No	Linear	Average voltage control	-	28V /8V	93.2% /97%
[63]	APFC	H-bridge (multiplexing switches)	-	P	Yes	Linear	Average current control	-	<0.1A	88%
[64]/[65]	DVRC	H-bridge	BPF	Current hysteresis control	No	Linear	Average voltage control	-	10V /12V	99.4% /98%
[66]/[67]	DVRC	H-bridge	BPF	-	No	Linear	Average voltage control	-	8.2V /9.2V	98.5% /94%
[68]/[69]	APFC	H-bridge	HPF	PID	No	Linear	Average voltage control	-	0.7A /0.15A	-/85%
[70]	APFC	Differential circuit	-	Multi-resonant (2,4,6 orders)	Yes	Linear	Waveform tracking	<1%	0.17A	91%
[71]	APFC	Differential circuit	-	P&O	Yes	Linear	Waveform tracking	-	0.156A	-
[72]-[74]	DVRC	Buck-boost	PR	P	Yes	Linear	Average voltage control	-	-/- /<5V	-/93% /96.48%
[75]/[76]	DVRC	Buck-boost	PR	P	Yes	Linear	Average voltage control	3% /1.7%	3V /2V	94.8% /-
[77]	APFC	Buck-boost	NF	TSMC	Yes	Non-Ideal Power Grid	Average voltage control	4.8%	5V	-
[78]	DVRC	Buck-boost	PR	PI	Yes	Linear	Average voltage control	-	-	96%

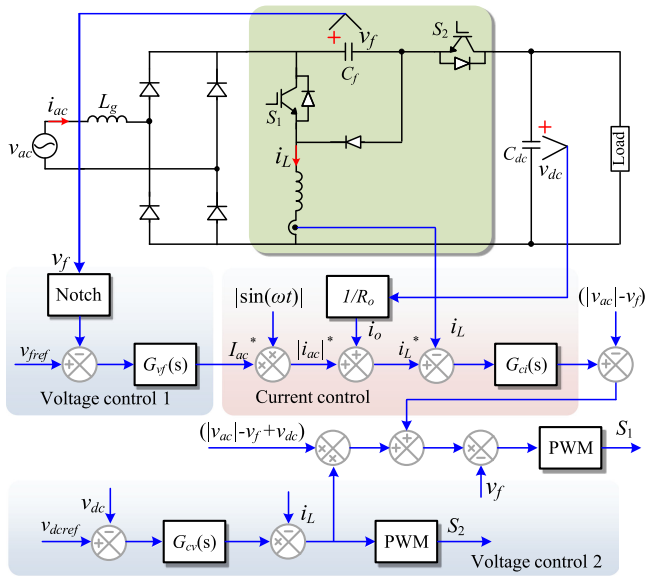

Fig. 13. Applying the CBBC method for the quasi-two-stage PFC circuit.

case, the decoupling circuit is a classic boost dc–dc circuit). In [89], [90], [93], and [94], the dual-loop control structure, in which the dc bus voltage $v_{\rm dc}$ is the outer loop and the current i_d in the decoupling circuit is the inner loop, is proposed to cope with the control challenge. In [95] and [96], to enhance the decoupling performance, the low-frequency ripple current is also extracted by a BPF and sent into a PR controller to generate an extra modulation voltage besides feeding back the output voltage error.

To tackle the coupling and the nonlinearity issues of the system and achieve fast transient response and large-signal stability, a nonlinear automatic-power-decoupling controller based on the input–output feedback linearization technique is developed [91]. The grid current $i_{\rm ac}$ and the dc bus voltage $v_{\rm dc}$ are controlled to track their respective references with zero steady-state errors with global stability. And the decoupling capacitor voltage is not directly controlled and taken as a zero dynamic. However, the proposed control is inapplicable when the decoupling circuit operates in CCM because the system is a nonminimum phase when the energy is transferred back to the dc bus [92], [97]. To solve the instability problem, an evolved automatic-power-decoupling controller that incorporates the Lyapunov direct control method is proposed [92]. The Lyapunov direct method is used to ensure $v_{\rm dc}$ and i_d converges to track their respective references. The decoupling capacitor voltage is stable according to the principle of the conservation of energy. In [97], the feedback linearization is applied to transform the system from current–voltage to the power-energy domain to both eliminate the instability and increase the voltage loop bandwidth. In [98], the nonlinear sliding-mode controller is developed to handle this problem. To improve the steady-state performance, a simple integrator of the output voltage error ($V_{\rm dcref}$–$V_{\rm dc}$) is added to the sliding function.

For some quasi-two-stage PFC circuits (an example is shown in Fig. 13), the CBBC principle is directly employed to achieve

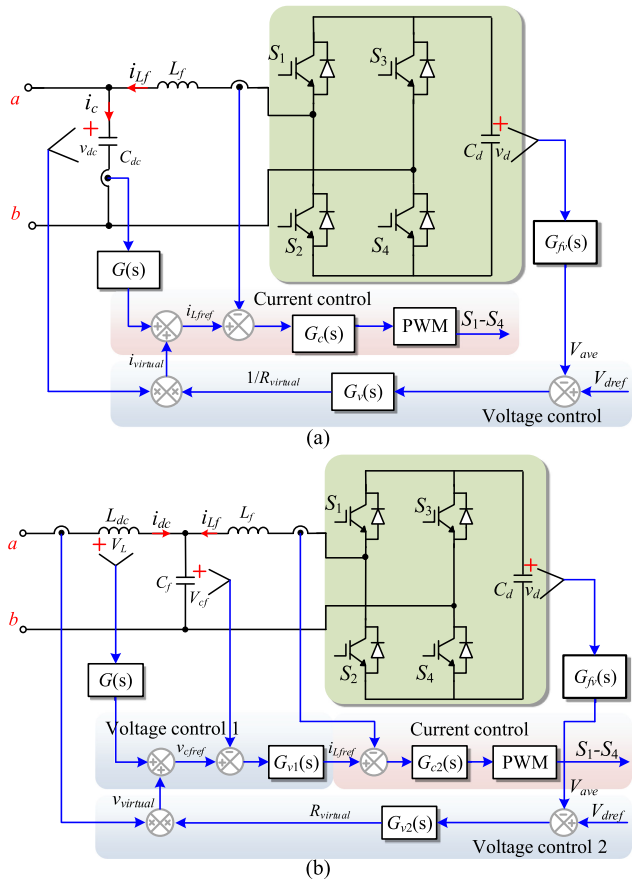

Fig. 14. Application examples of VIBC method. (a) CCCS method. (b) VCVS method.

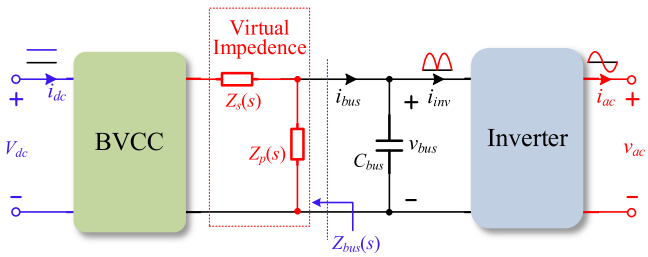

Fig. 15. Application example of VIBC method in two-stage single-phase converter by modifying the control structure.

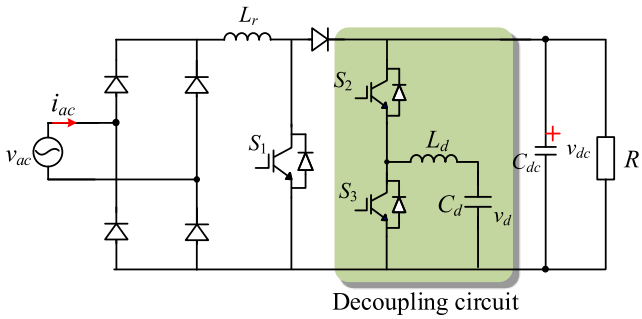

Fig. 16. Main circuit for performance testing.

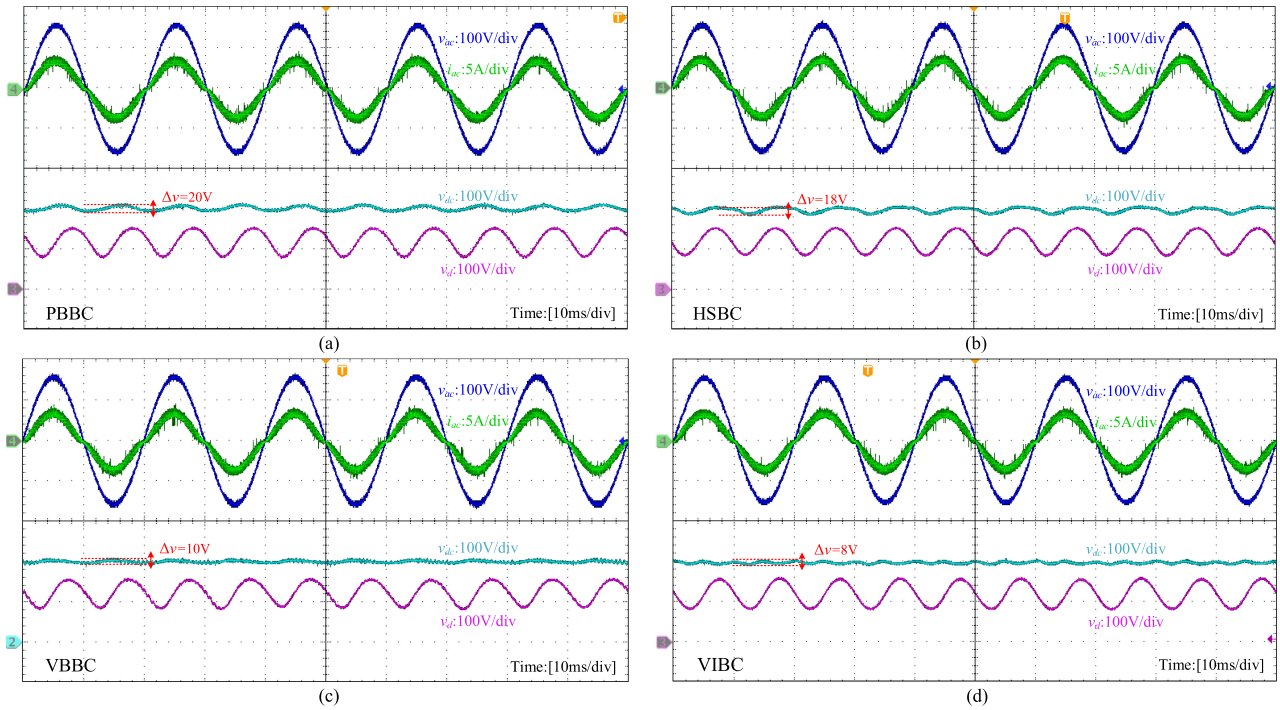

Fig. 17. Steady-state experimental waveforms when the dc-link voltage is 200 V with (a) PBBC, (b) HSBC, (c) VBBC, and (d) VIBC.

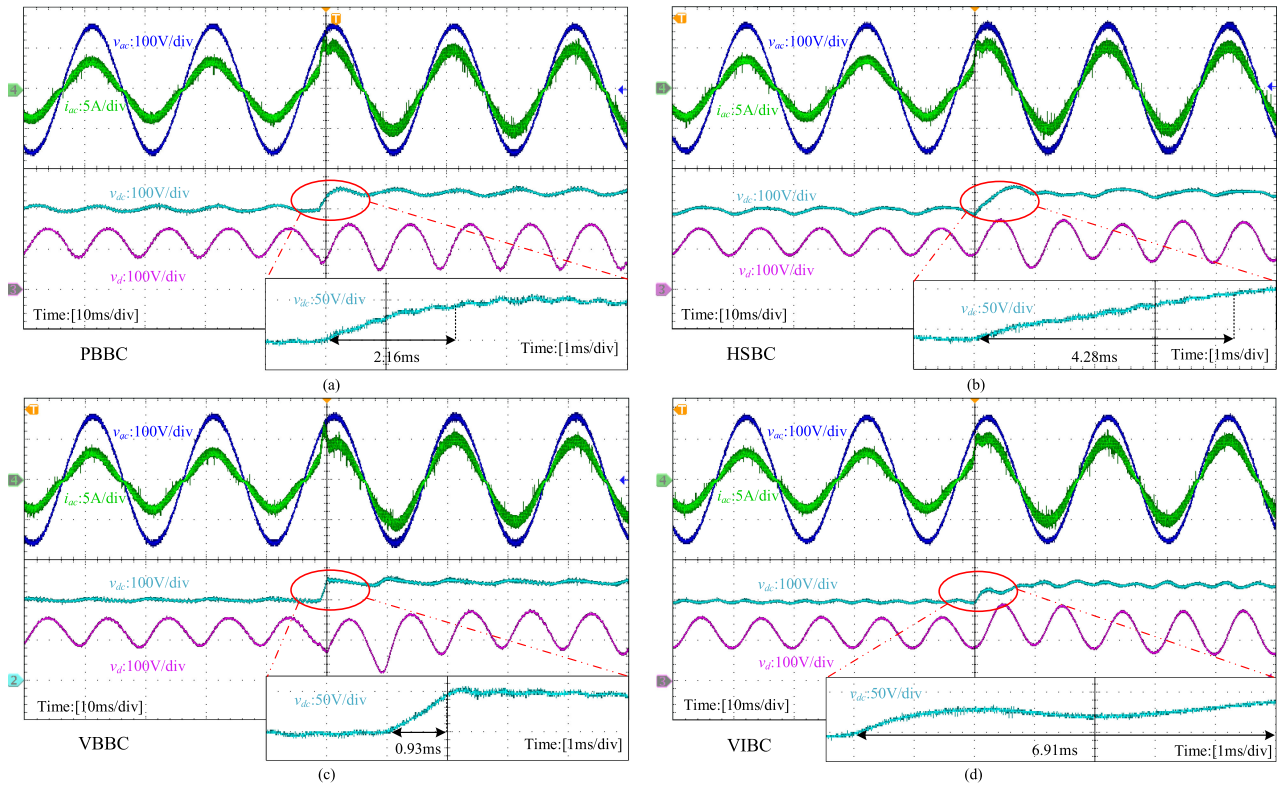

Fig. 18. Dynamic experimental waveforms considering a step change of the dc-link voltage from 200 to 245 V with (a) PBBC, (b) HSBC, (c) VBBC, and (d) VIBC.

TABLE III
SUMMARY OF VBBC/CBBC METHODS

Reference	Decoupling circuit	Close loop decoupling ?	Linear or nonlinear load	Decoupling voltage control	Feature	THD	DC link voltage /current ripple (peak-to-peak value)	Efficiency
[80]/[81]	Buck-boost	Yes	Linear	Peak voltage control	• Linear control • Voltage error and the ripple current are both fed back	4.63% /4.47%	1.2A /1A	80.5% /91%
[89]/[90]	Buck	Yes	Linear	Average voltage control	• Dual loop control	2%/-	11V /14V	92.5% /92.5%
[91]	Buck	Yes	Linear	Average voltage control	• Feedback linearization	3.57%	2V	-
[92]	Buck	Yes	Linear	Average voltage control	• Feedback linearization with direct Lyapunov control	0.6%	9V	-
[93]/[94]	Buck	Yes	Linear	Average voltage control	• Dual loop control	-	2V /14V	-
[95]/[96]	Buck-boost	Yes	Linear	Peak voltage control	• Linear control • Voltage error and the ripple current are both fed back	4% /4%	5V /2V	92.5% /93%
[97]	Buck	Yes	Linear	Average voltage control	• Feedback linearization control under power-energy domain	2.5%	14V	99.5%
[98]	Buck	Yes	Linear	Average voltage control	• SMC	0.72%	1.63V	-
[99]/[100]/[103]	Quasi two stage	Yes	Linear	Average voltage control	• Linear control	3.6% /2.7% /3.6%	5V/- /7.3V	-/95.5%/-
[101]	Quasi two stage	Yes	Linear	Average voltage control	• SMC	4.24%	<5V	90.3%
[102]	PFC	Yes	Linear	Average voltage control	• DCM for ac side and CCM for dc side • Switching frequency is a variable	3.5%	5V	89.5%
[105]	Buck	Yes	-	Average voltage control	• Linear control • No dedicated controller for v_d	-	3.3V	93%
[106]	Buck	Yes	Linear	Average voltage control	• Dual loop control • Predefined decoupling capacitor voltage	-	12V	-
[107]	Dual Half-Bridge	Yes	Linear	Average voltage control	• Using voltage information only • Independent of the inverter control • Phase shift control	-	20V	93.4%

the high-quality ac current and constant dc output voltage. And the ripple power is buffered by the intermediate capacitor [99]–[103]. Actually, for two-stage single-phase inverters (a dc–dc circuit cascaded with a dc/ac inverter), this control method is also widely used [104]. For this special circuit structure, the power flow is unidirectional, that is, it flows from the dc source to the decoupling capacitor and then the ac load. While, for the buck or boost decoupling circuit, the power sweeps between the dc link and the decoupling capacitor. In [101], the SMC scheme is applied to guarantee stability under the model uncertainties and nonlinearities in the power-decoupling circuit. For some PFCs with only one active switch, it is hard to handle the ac grid current and the constant output voltage at the same time. However, in [102], the CBBC is applied by taking the switching frequency as another control variable.

It is interesting that the CBBC method can be modified to own the novelty of having a plug-and-play operation [105]–[107]. In [105], only one dc bus voltage sensor is needed. And the decoupling circuit can be directly connected to and disconnected from the dc link without the need for modifying the host system as well as the communication network. The average value of the decoupling capacitor voltage is automatically maintained at half the dc bus voltage by adding a feedforward term of 0.5 to the modulation signal. Consequently, the decoupling circuit shows a nonintrusive property and hot swap performance. The main drawback is the need for the prior knowledge of the base frequencies of the pulsating voltage components for designing the multiresonant controller. In [106], a plug-and-play controller is designed without knowing the properties of the dc bus (such as the frequencies of the ripple voltage). The dc bus voltage reference V_{dcref} is not directly given but generated by the decoupling capacitor voltage (average value) error. If the generated V_{dcref} is equal to the real equilibrium voltage of the dc bus (called V_{real}), the decoupling capacitor voltage error will be zero. However, for example, if V_{dc} is smaller than V_{real}, more current i_h will flow toward the decoupling circuit, thus increasing v_d. Then, the decoupling capacitor voltage error would increase V_{dcref}. This process will continue until $V_{\mathrm{dcref}} = V_{\mathrm{real}}$. In this control, the average value of the decoupling capacitor voltage is predefined. In [107], a voltage-fed phase-shift dual half-bridge

TABLE IV
SUMMARY OF VIRTUAL IMPEDANCE BASED CONTROL METHODS

Reference	Decoupling circuit	Close loop decoupling?	Sampling	Plug-and-play	Decoupling voltage control	Feature	THD	DC link voltage /current ripple (peak-to-peak value)	Efficiency
[112]	H-bridge	Yes	i_{ca}, v_{dc}, i_c,v_d	Yes (for VSC)	Average voltage control	• Programmable power impedance	-	-	-
[113]	Buck	Yes	V_{dc}, v_d	Yes	Waveform tracking	• Active capacitor • Single loop control • DCM inductor current	-	7V	-
[114]	Buck	Yes	i_h, i_d, v_{dc}, v_a	Yes	Average voltage control	• Dual loop control • Varied dc bus voltage reference	2.1%	10V	99.7%
[115]	H-bridge	Yes	i_{dc}, v_l	Yes (for VSC)	Average voltage control	• Mimic an LC resonator	-	1A	84%

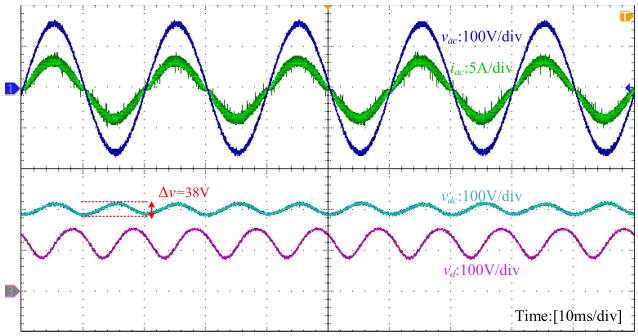

Fig. 19. Steady-state experimental waveforms with PBBC when calculating the decoupling voltage reference by changing the displacement angle from φ to $(\varphi+\pi/15)$.

(DHB) is employed as the decoupling circuit. A novel two-loop voltage-feedback controller is developed. One loop is for the dc-link ripple rejection and the other is to maintain the power-decoupling capacitor voltage at a specified average value. The outputs of the two control loops are added as the phase-shift angle. Then, no phase information is required, which makes the plug-and-play easy to realize.

C. Summary

Different from PBBC and HSBC control ideas, in which the decoupling circuits only handle the ripple voltage/current of the dc bus, VBBC/CBBC control is to directly regulate the dc bus current or voltage. It is a two-stage cascaded control structure in which the rectifier regulates the decoupling circuit capacitor voltage (regulating its average value) and the decoupling circuit maintains a stiff bus voltage/current (regulating its instantaneous value). This control concept is a closed-loop decoupling control and achieves excellent decoupling performance. In addition, this control has strong robustness since no precise reference is required. And the transient performance is also superior because the dc output voltage is tightly regulated by the decoupling circuit and the controller can be designed with a fast response [108]. As introduced before, this control concept is general and can be applied for various decoupling circuits with/without minor modification. However, the decoupling capacitor voltage needs to be unipolar with a certain dc component, storing a large portion of redundant energy. Therefore, the voltage utilization ratio is relatively low. What is worse, unstable and nonminimum phase circumstances will occur when the ripple power sweeps between the dc bus and the decoupling circuit that increases the difficulty of controller design. Besides, since the decoupling capacitor voltage fluctuates with a large range, the dc voltage regulation system is a time-varying linear system and the stability is hard to establish (linear matrix inequality or structured perturbation theory may be involved [98]).

V. VIBC METHOD

A. Control Idea

Usually, a large capacitor/inductor or an *LC* resonator tuned at $2f_{\rm ac}$ resonant frequency can be used to buffer the second-order ripple power. Up to now, this passive decoupling technique has been still widely used in PV [109], fuel cells [110], LED drivers [111], and so on. As well known, the output impedance of a two-terminal power electronic converter is controllable. Then, we can control the decoupling circuit to perform the behavior of a large capacitor/inductor or an *LC* resonator. From this aspect, some control schemes have been proposed [112]–[115].

B. Controller Schemes

In [112], the emulated power impedance is realized by mimic the exact voltage–current characteristic of a physical passive component. For the voltage-source-type converter, a current-controlled current-source (CCCS) method is used, as shown in Fig. 14(a). The low-frequency current in the dc bus filter capacitor is detected and magnified k-fold by $G_{v1}(s)$. The result is taken as the track reference of the decoupling circuit. Then, the decoupling circuit is equal to a capacitor with the value of $kC_{\rm dc}$. The extra term $i_{\rm virtual}$ is to compensate system losses. For the current-source-type converter, a voltage-controlled voltage-source (VCVS) method is used, as shown in Fig. 14(b). The low-frequency voltage in the dc bus filter inductor is detected and magnified k-fold by $G_{v1}(s)$. Similarly, the result will be the track reference of the decoupling circuit. Then, the decoupling circuit is equal to an inductor with the value of $kL_{\rm dc}$. In this method, the discontinuous current or voltage is sampled to avoid using a differentiator.

In [113], suppose $i_c = -ki_{ca}$ in Fig. 12, then the equivalent capacitance provided by the decoupling circuit is $kC_{\rm dc}$. The

TABLE V
COMPARISON BETWEEN THE FOUR CONTROL CONCEPTS

Terms	PBBC	HSBC	VBBC/CBBC	VIBC
Control of the original circuit	In charge of the average dc bus voltage/current	In charge of the average dc bus voltage/current	In charge of the average decoupling capacitor voltage	In charge of the average dc bus voltage/current
Control of the decoupling circuit	In charge of the decoupling capacitor voltage	In charge of the ripple voltage/current	Regulating the dc bus voltage/current	Emulating an impedance
Dependent with the original circuit control	No	No	Yes	No
Feedback the decoupling effect	No (Yes for some cases, see Table I)	No (Yes for some cases, see Table II)	Yes	Yes
Sensitive to system parameters	Yes	No	No	No
Plug and play	No	No	Yes for some cases, see Table III	Yes
Extra voltage loop to stabilize the decoupling voltage	No need	Need (No need for differential circuits, see Table II)	Need	Need
AC or DC decoupling voltage/current	AC or DC	DC	DC	DC
Complexity	Moderate (18.84 μs)*	Moderate (17.11 μs)	Low (16.19 μs)	Moderate (17.72 μs)
Decoupling performance	Good (20 V)**	Good (18 V)	Excellent (10 V)	Excellent (8 V)
Dynamic performance	Fair (2.16 ms)***	Poor (4.28 ms)	Good (0.93 ms)	Poor (6.91 ms)
Modularization	Fair	Fair	Hard	Easy

*18.84/17.11/16.19/17.72 μs is the execution time of each control method (including sampling, phase-locked loop, protection, and main program) in the physics experiment.
**20/18/10/8 V is the measured peak-to-peak value of dc bus voltage in a steady state.
***2.16/4.28/0.93/6.91 ms is the settling time of the dc bus voltage during the step change process.

decoupling capacitor voltage is expressed as

$$v_d^2 = k\frac{C_{\rm dc}}{C_d}v_{\rm dc}^2 + \text{constant}. \tag{8}$$

Note that the gain k is not a constant and varies with frequencies. It should be small at very low frequencies, which determines the average value of v_d. Within the frequency range of interest (the frequencies of the ripple currents), k needs to be large to mimic a sufficient capacitance. This control is an indirect approach in which the dc bus voltage is indirectly influenced after the square of the decoupling capacitor voltage (i.e., energy in the capacitor) is under control. The control structure is simple as only a single control loop is involved. The plug-and-play operation is allowed, as only the dc bus voltage information is needed to accomplish the control.

In [114], the decoupling circuit is supposed to mimic a large capacitor $C_{\rm mimic}$. Then, the dc voltage can be expressed as

$$v_{\rm dc}^*(t) = \frac{1}{C_{\rm mimic}}\int_{t_0}^{t} i_h(\tau) - i_0(\tau)d\tau + v_{\rm dc}(t_0) \tag{9}$$

where $i_0(\tau)$ is the loss compensating term to maintain the average decoupling capacitor voltage. Then, (9) is taken as the dc bus voltage reference regulated by the decoupling circuit. This control supports the desired plug-and-play operation since neither the circuit nor the control of the original circuit needs to be modified.

For single-phase current-source-type rectifiers, a physical passive *LC* resonator tuned at $2f_{\rm ac}$ resonant frequency can be inserted into the dc bus to block the ripple voltage flowing into the dc side. Obviously, the size of the resonator will be large as a result of the low resonant frequency. Inspired by this, in [115], the decoupling circuit is controlled to emulate the external voltage characteristic of an *LC* tank circuit. Then, the same function as a real *LC* tank circuit can be achieved. This active *LC* emulator also overcomes the drawback of the *LC* parameter drifts in the passive case, which will degrade the decoupling performance. This method can be applied in both the current-source converter (emulating a series *LC* resonator to block the low-frequency ripple voltage) and the voltage-source converter (emulating a parallel *LC* resonator to bypass the low-frequency ripple current).

For two-stage single-phase converters, the virtual-impedance-based approach can be directly applicable by only modifying the control structure. As seen in Fig. 15, a virtual series impedance $Z_s(s)$ and parallel impedance $Z_p(s)$ with high impedance at the ripple frequency and low impedance at the rest of the frequencies are introduced. Then, the ripple power is prevented from entering the dc side and buffered by the dc bus capacitor with a relatively large voltage fluctuation. The various schemes for realizing the virtual impedance have been analyzed and compared in [104]. The highlight of this control is to realize the virtual impedance without adding extra decoupling circuits.

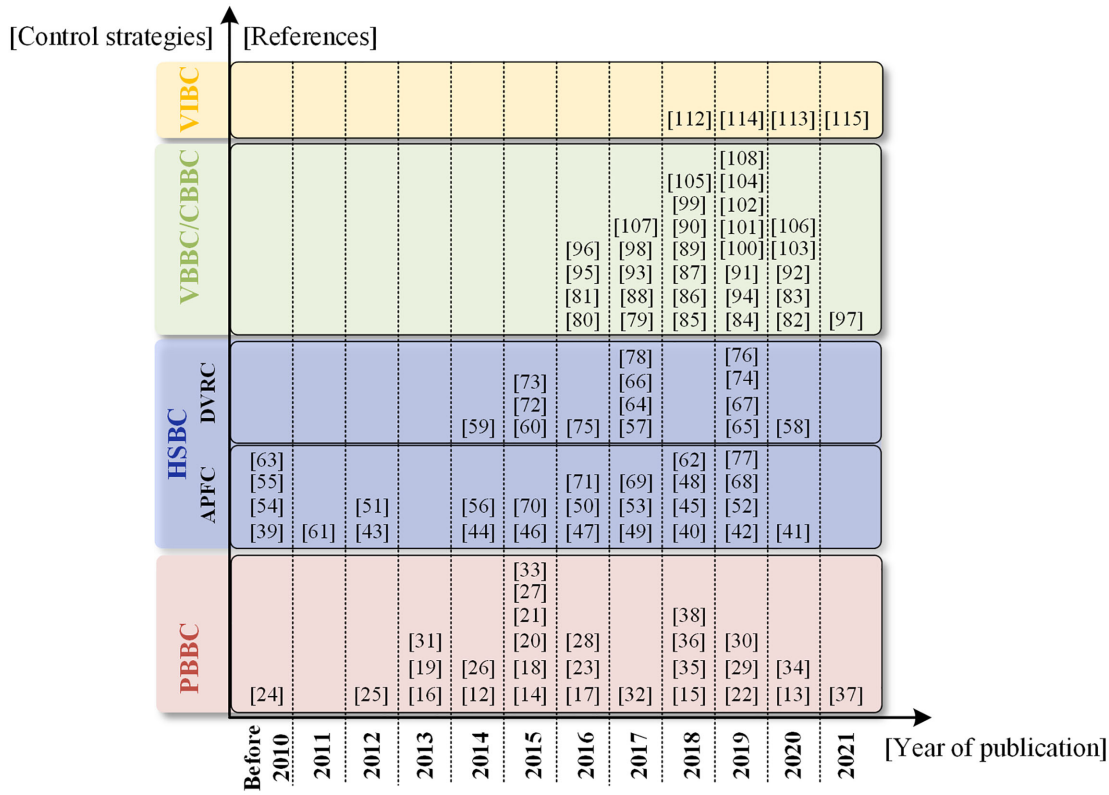

Fig. 20. Historical overview of control strategies for APD.

However, the applications of this control are limited due to the dependence on circuit structure.

C. Summary

VIBC achieves the power decoupling by emulating the voltage or current characteristic of the passive components. The 2ω ripple power is thought to be well handled if the accurate emulation is realized. Actually, this is an indirect decoupling method and the decoupling effects are determined by the emulation accuracy. The decoupling circuit can be linked to the host system through the dc link directly and no intrusive sensors and central controllers are required. Consequently, this control idea is easy to achieve plug-and-play operation. Different implementations based on the VIBC are summarized in Table IV. For the proposed strategies in [112] and [114], four sensor circuits are required. However, in [113] and [115], the required sensors are reduced and the cost can be saved.

However, the dynamic performances in [112] and [114] are superior to those in [113] and [115]. This is because a resonant controller [115] and an LPF [113] are, respectively, involved.

VI. Experimental Case Study

In order to assess the performance of the four different control concepts, a benchmark case study is established. For a fair comparison, the same rectifier, as defined in Fig. 16, is used in all the tests. It is consisted of a widely used boost PFC circuit and a buck decoupling circuit. The grid voltage is 110 $V_{\rm RMS}$/50 Hz, L_r and L_d are 3.6 and 1.5 mH, C_d and $C_{\rm dc}$ are 100 and 30 μF, the output voltage is 200 V, and the load R is 200 Ω. And the switching frequency is 20 kHz.

The experimental waveforms from the different tests are shown in Figs. 17–19. On the basis of the obtained results, the following comments can be made.

1) Good input and output performances are achieved in the four control ideas. The output dc-link voltages are smooth as the low-frequency ripple power is buffered by the decoupling capacitor.
2) The decoupling performance of VBBC and VIBC is superior compared with PBBC and HSBC. Therefore, it can be found that the peak-to-peak value of the dc-link voltage presented in VBBC and VIBC is smaller than that in PBBC and HSBC. The reason is that, in PBBC and HSBC, the decoupling control is an open loop in essence due to the fact that the decoupling effect is not fed back.
3) For the dynamic performance test, the output voltage reference is suddenly increased to be 245 V. Considering a step change of the dc-link voltage, the settling time is only 0.93 ms for VBBC. However, it is 2.16 ms/4.28 ms/6.91 ms for PBBC/HSBC/VIBC, respectively. The reason is that the dc output voltage is tightly regulated by the decoupling circuit.
4) For PBBC, its decoupling performance is sensitive to system parameters. As shown in Figs. 17(a) and 19, the dc-link voltage deteriorates (the peak-to-peak value of the dc-link voltage is increased to 38 V) when the decoupling voltage reference is calculated by changing the displacement angle from φ to (φ+π/15).

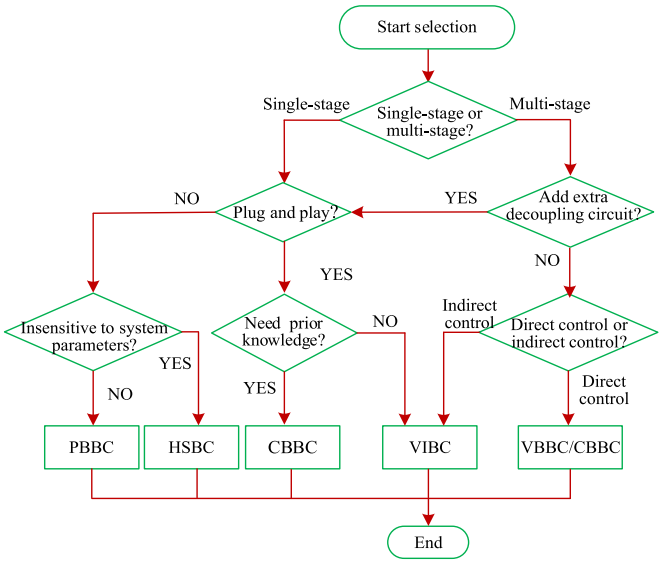

Fig. 21. General guidelines for selecting a proper control method for APD.

VII. Discussion and Conclusion

The operation principles, characteristics, and features of the proposed control methods in the literature for APD are introduced, explained, and compared in this article. These control methods are classified based on the control ideas, namely "power balance," "harmonic suppression," "volt-second balance/charge balance," and "virtual impedance." Taking the application of rectification as an example, the features of the four control ideas are summarized in Table V.

For PBBC, the original circuit is controlled to regulate the average dc bus voltage/current and the decoupling circuit is controlled to track the decoupling capacitor voltage reference. The highlights are easy implementation and independent controller design with the original circuit. In addition, the decoupling capacitor voltage can be ac waveform that makes the voltage utilization ratio reach 100%. While, in other control ideas, the decoupling capacitor voltage includes a dc component and the voltage utilization ratio is lower. Also, an extra voltage control loop is not required to stabilize the decoupling capacitor voltage, which is needed to maintain the average decoupling capacitor voltage in other control ideas. However, the decoupling effects are fair due to the strong dependence of parameters and usual open-loop decoupling control. A center controller is also preferred since the information of the phase angle and power of the original circuit is needed when determining the decoupling voltage/current reference.

For HSBC, the original circuit is controlled to regulate the average dc bus voltage/current and the decoupling circuit is controlled to provide an adequate counteraction voltage/current to ensure a constant dc bus current/voltage. Many mature control strategies in the field of harmonic suppression can be adopted with a minor modification. In the DVRC case, the decoupling circuit only handles a part of the ripple power (only 8.4% [64]), which reduces the efficiency penalty. Compared with other control ideas, an additional modification on the original circuit is needed to add a current sensor or a series capacitor with the dc bus, which is adverse to the modular design. What is worse, such as PBBC, the decoupling performance is not fed back to the control loop and a perfect power decoupling is hard to achieve. However, different from PBBC, it is immune to parameter drifts since the compensated voltage or current is extracted by sensor circuits in real time.

For VBBC/CBBC, the control structure is notably different from those in the other control ideas. The original circuit is in charge of the average decoupling capacitor voltage and the decoupling circuit is controlled to regulate the dc bus voltage tightly. This control idea makes the controls of the original circuit and the decoupling circuit coupled tightly. From the power flow viewpoint, the power can be the first thought to flow from the source to the decoupling capacitor (intermediate capacitor) and then to the load. Therefore, this control idea can be directly applied for two-stage or quasi-two-stage conversion circuits (the decoupling capacitor voltage is taken as the intermediate bus voltage) [99]–[104]. This control idea possesses superior decoupling performance and dynamic response since the dc bus voltage is directly regulated by the decoupling circuit. In addition, this control idea has a strong robustness to parameter variations since no precise voltage/current reference (decoupling voltage or compensated voltage/current) is needed. However, the modular design is difficult to achieve because the control structure of the original circuit needs to be changed in this control idea.

For VIBC, the original circuit is in charge of the average dc bus voltage/current and the decoupling circuit is controlled to emulate an impedance. The merit over other control ideas is the interesting function of plug-and-play operation since neither the power stage nor the control circuitry of the original circuit needs to be modified. Then, the modularization of the decoupling circuit is easy to realize. However, this control idea needs more high-precision current sensor circuits to detect the current flowing through the dc capacitor [112], [114]. Without employing extra sensors, the controller should be elaborately designed to magnify the factor k only within the frequency range of interest and avoid large phase distortion [113]. And the complexity of this controller will be increased when dealing with some cases, such as ripple power with multiple frequencies.

Moreover, a historical overview of the power-decoupling methods is shown in Fig. 20. The vertical axis is the control idea of the proposed power-decoupling methods. And the horizontal axis is the time (year) of the reference published. It is revealed that during the early period, the control strategies are developed mainly based on PBBC and HSBC. The reason may be that the PBBC is intuitive and easy to realize, and the mature control arts in the field of harmonic suppressing provide great enlightenment for HSBC. However, in recent years, VBBC/CBBC and VIBC have gained more attention due to the outstanding decoupling performance and/or plug-and-play operation.

Based on the preceding analysis, some general guidelines are suggested and shown in the flowchart of Fig. 21. The designer can select an appropriate control according to the given application.

In conclusion, further research works on the following subjects are expected.

1) Nearly all the developed control strategies are based on the linear loads and/or under ideal grid voltage. New control and management strategies need to be developed to handle the complex operation circumstances, such as pulsating loads, nonideal grid voltage (with large background harmonics), and ripple power with multiple frequencies (for example, single-phase ac–dc–ac drive system).
2) For the PBBC control idea, the existing control strategies are mostly designed based on the open-loop calculation. The closed-loop decoupling control is difficult because both the amplitude (V_d or A) and the phase shift (θ or φ) should be carefully modified at the same time. There is still much space for new control strategies to be developed.
3) Stability is crucial in a power electronics system. However, it is not clear how the system stability is affected by the added decoupling circuit. Especially for the VBBC/CBBC control means, the decoupling control and the original circuit control are strongly coupled.
4) For nearly all the control strategies, the controllers for the original circuit and the decoupling circuit are separate. A coordinated controller can be developed to achieve extra performance benefits, such as reducing the voltage ripple and switching times (for the switch-multiplexing decoupling circuit).

REFERENCES

[1] W. Li, Y. Gu, H. Luo, W. Cui, X. He, and C. Xia, "Topology review and derivation methodology of single-phase transformerless photovoltaic inverters for leakage current suppression," *IEEE Trans. Ind. Electron.*, vol. 62, no. 7, pp. 4537–4551, Jul. 2015.

[2] S. Li, S.-C. Tan, C. K. Lee, E. Waffenschmidt, S. Y. Hui, and C. K. Tse, "A survey, classification, and critical review of light-emitting diode drivers," *IEEE Trans. Power Electron.*, vol. 31, no. 2, pp. 1503–1516, Feb. 2016.

[3] M. Yilmaz and P. T. Krein, "Review of battery charger topologies, charging power levels, and infrastructure for plug-in electric and hybrid vehicles," *IEEE Trans. Power Electron.*, vol. 28, no. 5, pp. 2151–2169, May 2013.

[4] Y. Sun, Y. Liu, M. Su, W. Xiong, and J. Yang, "Review of active power decoupling topologies in single-phase systems," *IEEE Trans. Power Electron.*, vol. 31, no. 7, pp. 4778–4794, Jul. 2016.

[5] K. A. Kim, Y.-C. Liu, M.-C. Chen, and H.-J. Chiu, "Opening the box: Survey of high power density inverter techniques from the little box challenge," *CPSS Trans. Power Electron. Appl.*, vol. 2, no. 2, pp. 131–139, Jun. 2017.

[6] M. A. Vitorino, L. F. S. Alves, R. Wang, and M. B. de Rossiter Correa, "Low-frequency power decoupling in single-phase applications: A comprehensive overview," *IEEE Trans. Power Electron.*, vol. 32, no. 4, pp. 2892–2912, Apr. 2017.

[7] H. Hu, S. Harb, N. Kutkut, L. Batarseh, and Z. J. Shen, "A review of power decoupling techniques for microinverters with three different decoupling capacitor locations in PV systems," *IEEE Trans. Power Electron.*, vol. 28, no. 6, pp. 2711–2726, Jun. 2013.

[8] J. Zhang, H. Ding, B. Wang, X. Guo, and S. Padmanaban, "Active power decoupling for current source converters: An overview scenario," *Electronics*, vol. 8, no. 2, Feb. 2019, Art. no. 197.

[9] Y. Liu, B. Ge, H. Abu-Rub, and F. Blaabjerg, "Single-phase Z-source/quasi-Z-source inverters and converters: An overview of double-line-frequency power-decoupling methods and perspectives," *IEEE Ind. Electron. Mag.*, vol. 12, no. 2, pp. 6–23, Jun. 2018.

[10] Y. Zhan, Y. Guo, J. Zhu, L. Li, B. Yang, and B. Liang, "A review on mitigation technologies of low frequency current ripple injected into fuel cell and a case study," *Int. J. Hydrogen Energy*, vol. 45, no. 46, pp. 25167–25190, Sep. 2020.

[11] Z. Qin, Y. Tang, P. C. Loh, and F. Blaabjerg, "Benchmark of AC and DC active power decoupling circuits for second-order harmonic mitigation in kilowatt-scale single-phase inverters," *IEEE J. Emerg. Sel. Topics Power Electron.*, vol. 4, no. 1, pp. 15–25, Mar. 2016.

[12] M. Su, P. Pan, X. Long, Y. Sun, and J. Yang, "An active power-decoupling method for single-phase AC–DC converters," *IEEE Trans. Ind. Inform.*, vol. 10, no. 1, pp. 461–468, Feb. 2014.

[13] H. Rezaie, A. Khoshsaadat, J. S. Moghani, and H. Rastegar, "A new fluctuating power decoupling method based on ANFIS and PR control structures applicable to single-phase PWM rectifiers," *J. Eng. Res.*, vol. 8, no. 1, pp. 211–230, Mar. 2020.

[14] H. Han, Y. Liu, Y. Sun, M. Su, and W. Xiong, "Single-phase current source converter with power decoupling capability using a series-connected active buffer," *IET Power Electron.*, vol. 8, no. 5, pp. 700–707, May 2015.

[15] H. Watanabe, T. Sakuraba, K. Furukawa, K. Kusaka, and J.-I. Itoh, "Development of DC to single-phase AC voltage source inverter with active power decoupling based on flying capacitor DC/DC converter," *IEEE Trans. Power Electron.*, vol. 33, no. 6, pp. 4992–5004, Jun. 2018.

[16] S. Harb, M. Mirjafari, and R. S. Balog, "Ripple-port module-integrated inverter for grid-connected PV applications," *IEEE Trans. Ind. Appl.*, vol. 49, no. 6, pp. 2692–2698, Nov./Dec. 2013.

[17] G.-R. Zhu, H. Wang, B. Liang, S.-C. Tan, and J. Jiang, "Enhanced single-phase full-bridge inverter with minimal low-frequency current ripple," *IEEE Trans. Ind. Electron.*, vol. 63, no. 2, pp. 937–943, Feb. 2016.

[18] S. Li, G.-R. Zhu, S.-C. Tan, and S. Y. Hui, "Direct AC/DC rectifier with mitigated low-frequency ripple through inductor-current waveform control," *IEEE Trans. Power Electron.*, vol. 30, no. 8, pp. 4336–4348, Aug. 2015.

[19] G.-R. Zhu, S.-C. Tan, Y. Chen, and C. K. Tse, "Mitigation of low-frequency current ripple in fuel-cell inverter systems through waveform control," *IEEE Trans. Power Electron.*, vol. 28, no. 2, pp. 779–792, Feb. 2013.

[20] Y. Tang, F. Blaabjerg, P. C. Loh, C. Jin, and P. Wang, "Decoupling of fluctuating power in single-phase systems through a symmetrical half-bridge circuit," *IEEE Trans. Power Electron.*, vol. 30, no. 4, pp. 1855–1865, Apr. 2015.

[21] W. Cai, L. Jiang, B. Liu, S. Duan, and C. Zou, "A power decoupling method based on four-switch three-port DC/DC/AC converter in DC microgrid," *IEEE Trans. Ind. Appl.*, vol. 51, no. 1, pp. 336–343, Jan./Feb. 2015.

[22] M. Chingwena, T. Mouton, and M. Dorfling, "Model predictive control of an active capacitor for ripple energy compensation in single-phase DC-to-AC converters," in *Proc. Eur. Conf. Power Electron. Appl.*, 2019, pp. 1–10.

[23] H. Wu, S.-C. Wong, C. K. Tse, and Q. Chen, "Control and modulation of bidirectional single-phase AC–DC three-phase-leg SPWM converters with active power decoupling and minimal storage capacitance," *IEEE Trans. Power Electron.*, vol. 31, no. 6, pp. 4226–4240, Jun. 2016.

[24] T. Larsson and S. Ostlund, "Active DC link filter for two frequency electric locomotives," in *Proc. Int. Conf. Electr. Railways United Europe*, Amsterdam, The Netherlands, 1995, pp. 97–100.

[25] Z. Chen, C. Ling, F. Ye, and L. Ge, "A single-phase grid-connected inverter with an active power decoupling circuit," in *Proc. 24th Chin. Control Decis. Conf.*, Taiyuan, China, 2012, pp. 2806–2810.

[26] Y. Ohnuma and J.-I. Itoh, "A novel single-phase buck PFC AC–DC converter with power decoupling capability using an active buffer," *IEEE Trans. Ind. Appl.*, vol. 50, no. 3, pp. 1905–1914, May/Jun. 2014.

[27] Y. Ohnuma, K. Orikawa, and J.-I. Itoh, "A single-phase current-source PV inverter with power decoupling capability using an active buffer," *IEEE Trans. Ind. Appl.*, vol. 51, no. 1, pp. 531–538, Jan./Feb. 2015.

[28] A. S. Morsy and P. N. Enjeti, "Comparison of active power decoupling methods for high-power-density single-phase inverters using wide-bandgap FETs for google little box challenge," *IEEE J. Emerg. Sel. Topics Power Electron.*, vol. 4, no. 3, pp. 790–798, Sep. 2016.

[29] Z. Liang, S. Hu, and X. He, "Analysis and suppression strategy for the double-line frequency pulsation in single-phase quasi-Z-source converter," *IEEE Trans. Power Electron.*, vol. 34, no. 12, pp. 12567–12576, Dec. 2019.

[30] C. C. D. Viana, T. Soong, and P. W. Lehn, "Single-input space vector based control system for ripple mitigation on single-phase converters," *IEEE Trans. Power Electron.*, vol. 34, no. 4, pp. 3765–3774, Apr. 2019.

[31] H. Li, K. Zhang, H. Zhao, S. Fan, and J. Xiong, "Active power decoupling for high-power single-phase PWM rectifiers," *IEEE Trans. Power Electron.*, vol. 28, no. 3, pp. 1308–1319, Mar. 2013.

[32] R. Chen, Y. Liu, and F. Z. Peng, "A solid state variable capacitor with minimum capacitor," *IEEE Trans. Power Electron.*, vol. 32, no. 7, pp. 5035–5044, Jul. 2017.

[33] R. Chen, Y. Liu, and F. Z. Peng, "DC capacitor-less inverter for single-phase power conversion with minimum voltage and current stress," *IEEE Trans. Power Electron.*, vol. 30, no. 10, pp. 5499–5507, Oct. 2015.

[34] X. Wang, M. Chen, B. Li, and N. Chen, "Multifunction control strategy for single-phase AC/DC power conversion systems with voltage-sensorless power-decoupling function," *IEEE Trans. Power Electron.*, vol. 35, no. 12, pp. 13602–13620, Dec. 2020.

[35] S. Xu, R. Shao, L. Chang, and M. Mao, "Single-phase differential buck–boost inverter with pulse energy modulation and power decoupling control," *IEEE J. Emerg. Sel. Topics Power Electron.*, vol. 6, no. 4, pp. 2060–2072, Dec. 2018.

[36] S. Komeda and H. Fujita, "A power decoupling control method for an isolated single-phase AC-to-DC converter based on direct AC-to-AC converter topology," *IEEE Trans. Power Electron.*, vol. 33, no. 11, pp. 9691–9698, Nov. 2018.

[37] S. Xu, B. Cao, L. Chang, and R. Shao, "Pulse energy modulation for a single-phase bridge inverter with active power decoupling capability," *IEEE J. Emerg. Sel. Topics Power Electron.*, vol. 9, no. 2, pp. 2014–2026, Apr. 2021.

[38] B. Ge *et al.*, "Direct instantaneous ripple power predictive control for active ripple decoupling of single-phase inverter," *IEEE Trans. Ind. Electron.*, vol. 65, no. 4, pp. 3165–3175, Apr. 2018.

[39] J.-I. Itoh and F. Hayashi, "Ripple current reduction of a fuel cell for a single-phase isolated converter using a DC active filter with a center tap," *IEEE Trans. Power Electron.*, vol. 25, no. 3, pp. 550–556, Mar. 2010.

[40] N. Takaoka, H. Takahashi, and J.-I. Itoh, "Isolated single-phase matrix converter using center-tapped transformer for power decoupling capability," *IEEE Trans. Ind. Appl.*, vol. 54, no. 2, pp. 1523–1531, Mar./Apr. 2018.

[41] X. Ren, L. Bai, Y. Chen, Z. Zhang, and Q. Chen, "Single-phase AC–DC converter with SiC power pulsation buffer for pulse load applications," *IEEE J. Emerg. Sel. Topics Power Electron.*, vol. 8, no. 1, pp. 517–528, Mar. 2020.

[42] P. Fang, S. Webb, Y.-F. Liu, and P. C. Sen, "Single-stage LED driver achieves electrolytic capacitor-less and flicker-free operation with unidirectional current compensator," *IEEE Trans. Power Electron.*, vol. 34, no. 7, pp. 6760–6776, Jul. 2019.

[43] Q.-C. Zhong, W.-L. Ming, X. Cao, and M. Krstic, "Reduction of DC-bus voltage ripples and capacitors for single-phase PWM-controlled rectifiers," in *Proc. 38th Annu. Conf. IEEE Ind. Electron. Soc.*, 2012, pp. 708–713.

[44] Y. Yang, X. Ruan, L. Zhang, J. He, and Z. Ye, "Feed-forward scheme for an electrolytic capacitor-less AC/DC LED driver to reduce output current ripple," *IEEE Trans. Power Electron.*, vol. 29, no. 10, pp. 5508–5517, Oct. 2014.

[45] X. Huang, X. Ruan, F. Du, F. Liu, and L. Zhang, "A pulsed power supply adopting active capacitor converter for low-voltage and low-frequency pulsed loads," *IEEE Trans. Power Electron.*, vol. 33, no. 11, pp. 9219–9230, Nov. 2018.

[46] X. Cao, Q.-C. Zhong, and W.-L. Ming, "Ripple eliminator to smooth DC-bus voltage and reduce the total capacitance required," *IEEE Trans. Ind. Electron.*, vol. 62, no. 4, pp. 2224–2235, Apr. 2015.

[47] Y. Tang, W. Yao, P. C. Loh, and F. Blaabjerg, "Highly reliable transformerless photovoltaic inverters with leakage current and pulsating power elimination," *IEEE Trans. Ind. Electron.*, vol. 63, no. 2, pp. 1016–1026, Feb. 2016.

[48] L. Zhang, X. Ruan, and X. Ren, "One-cycle control for electrolytic capacitor-less second harmonic current compensator," *IEEE Trans. Power Electron.*, vol. 33, no. 2, pp. 1724–1739, Feb. 2018.

[49] Q.-C. Zhong, W.-L. Ming, W. Sheng, and Y. Zhao, "Beijing converters: Bridge converters with a capacitor added to reduce leakage currents, DC-bus voltage ripples, and total capacitance required," *IEEE Trans. Ind. Electron.*, vol. 64, no. 1, pp. 325–335, Jan. 2017.

[50] D. B. W. Abeywardana, B. Hredzak, and V. G. Agelidis, "An input current feedback method to mitigate the DC-side low-frequency ripple current in a single-phase boost inverter," *IEEE Trans. Power Electron.*, vol. 31, no. 6, pp. 4594–4603, Jun. 2016.

[51] S. Wang, X. Ruan, K. Yao, S.-C. Tan, Y. Yang, and Z. Ye, "A flicker-free electrolytic capacitor-less AC–DC LED driver," *IEEE Trans. Power Electron.*, vol. 27, no. 11, pp. 4540–4548, Nov. 2012.

[52] W. Yao, Y. Xu, Y. Tang, P. C. Loh, X. Zhang, and F. Blaabjerg, "Generalized power decoupling control for single-phase differential inverters with nonlinear loads," *IEEE J. Emerg. Sel. Topics Power Electron.*, vol. 7, no. 2, pp. 1137–1151, Jun. 2019.

[53] W. Yao, X. Wang, P. C. Loh, X. Zhang, and F. Blaabjerg, "Improved power decoupling scheme for a single-phase grid-connected differential inverter with realistic mismatch in storage capacitances," *IEEE Trans. Power Electron.*, vol. 32, no. 1, pp. 186–199, Jan. 2017.

[54] I. Serban and C. Marinescu, "Active power decoupling circuit for a single-phase battery energy storage system dedicated to autonomous microgrids," in *Proc. IEEE Int. Symp. Ind. Electron.*, 2010, pp. 2717–2722.

[55] R.-J. Wai and C.-Y. Lin, "Active low-frequency ripple control for clean-energy power-conditioning mechanism," *IEEE Trans. Ind. Electron.*, vol. 57, no. 11, pp. 3780–3792, Nov. 2010.

[56] W. Cai, B. Liu, S. Duan, and L. Jiang, "An active low-frequency ripple control method based on the virtual capacitor concept for BIPV systems," *IEEE Trans. Power Electron.*, vol. 29, no. 4, pp. 1733–1745, Apr. 2014.

[57] P. Fang and Y.-F. Liu, "Energy channeling LED driver technology to achieve flicker-free operation with true single stage power factor correction," *IEEE Trans. Power Electron.*, vol. 32, no. 5, pp. 3892–3907, May 2017.

[58] P. Yang, J. Cao, Z. Shang, Y. Cai, and J. Xu, "Double-line frequency ripple suppression of a quasi-single stage AC-DC converter," *IEEE Trans. Circuits Syst. II, Express Briefs*, vol. 67, no. 10, pp. 2074–2078, Oct. 2020.

[59] H. Wang, H. S.-H. Chung, and W. Liu, "Use of a series voltage compensator for reduction of the DC-link capacitance in a capacitor-supported system," *IEEE Trans. Power Electron.*, vol. 29, no. 3, pp. 1163–1175, Mar. 2014.

[60] W. Liu, K. Wang, H. S.-H. Chung, and S. T.-H. Chuang, "Modeling and design of series voltage compensator for reduction of DC-link capacitance in grid-tie solar inverter," *IEEE Trans. Power Electron.*, vol. 30, no. 5, pp. 2534–2548, May 2015.

[61] R. Wang *et al.*, "A high power density single-phase PWM rectifier with active ripple energy storage," *IEEE Trans. Power Electron.*, vol. 26, no. 5, pp. 1430–1443, May 2011.

[62] H. V. Nguyen and D.-C. Lee, "Reducing the DC-link capacitance: A bridgeless PFC boost rectifier that reduces the second-order power ripple at the DC output," *IEEE Ind. Appl. Mag.*, vol. 24, no. 2, pp. 23–34, Mar./Apr. 2018.

[63] T. Shimizu, Y. Jin, and G. Kimura, "DC ripple current reduction on a single-phase PWM voltage-source rectifier," *IEEE Trans. Ind. Appl.,* vol. 36, no. 5, pp. 1419–1429, Sep./Oct. 2000.

[64] S. Qin, Y. Lei, C. Barth, W.-C. Liu, and R. C. N. Pilawa-Podgurski, "A high power density series-stacked energy buffer for power pulsation decoupling in single-phase converters," *IEEE Trans. Power Electron.*, vol. 32, no. 6, pp. 4905–4924, Jun. 2017.

[65] X. Lyu, N. Ren, and D. Cao, "Instantaneous pulse power compensator for high-density single-phase inverters," *IEEE Trans. Power Electron.*, vol. 34, no. 11, pp. 10776–10785, Nov. 2019.

[66] H. Wang and Huai Wang, "A two-terminal active capacitor," *IEEE Trans. Power Electron.*, vol. 32, no. 8, pp. 5893–5896, Aug. 2017.

[67] H. Wang, Y. Liu, and Huai Wang, "On the practical design of a two-terminal active capacitor," *IEEE Trans. Power Electron.*, vol. 34, no. 10, pp. 10006–10020, Oct. 2019.

[68] H. Wang and Huai Wang, "A two-terminal active inductor with minimum apparent power for the auxiliary circuit," *IEEE Trans. Power Electron.*, vol. 34, no. 2, pp. 1013–1016, Feb. 2019.

[69] J. He, X. Ruan, and L. Zhang, "Adaptive voltage control for bidirectional converter in flicker-free electrolytic capacitor-less AC-DC LED driver," *IEEE Trans. Ind. Electron.*, vol. 64, no. 1, pp. 320–324, Jan. 2017.

[70] I. Serban, "Power decoupling method for single-phase H-bridge inverters with no additional power electronics," *IEEE Trans. Ind. Electron.*, vol. 62, no. 8, pp. 4805–4813, Aug. 2015.

[71] D. B. W. Abeywardana, B. Hredzak, and V. G. Agelidis, "A rule-based controller to mitigate DC-side second-order harmonic current in a single-phase boost inverter," *IEEE Trans. Power Electron.*, vol. 31, no. 2, pp. 1665–1679, Feb. 2016.

[72] Y. Tang, Z. Qin, F. Blaabjerg, and P. C. Loh, "A dual voltage control strategy for single-phase PWM converters with power decoupling function," *IEEE Trans. Power Electron.*, vol. 30, no. 12, pp. 7060–7071, Dec. 2015.

[73] Y. Tang and F. Blaabjerg, "A component-minimized single-phase active power decoupling circuit with reduced current stress to semiconductor switches," *IEEE Trans. Power Electron.*, vol. 30, no. 6, pp. 2905–2910, Jun. 2015.

[74] J. Roy, Y. Xia, and R. Ayyanar, "Half-bridge voltage swing inverter with active power decoupling for single-phase PV systems supporting wide power factor range," *IEEE Trans. Power Electron.*, vol. 34, no. 8, pp. 7450–7461, Aug. 2019.

[75] S. Li, W. Qi, S.-C. Tan, and S. Y. Hui, "Integration of an active filter and a single-phase AC/DC converter with reduced capacitance requirement

and component count," *IEEE Trans. Power Electron.*, vol. 31, no. 6, pp. 4121–4137, Jun. 2016.

[76] K.-P. Huang, Y. Wang, and R.-J. Wai, "Design of power decoupling strategy for single-phase grid-connected inverter under nonideal power grid," *IEEE Trans. Power Electron.*, vol. 34, no. 3, pp. 2938–2955, Mar. 2019.

[77] Y. Wang and R.-J. Wai, "Adaptive power decoupling strategy for single-phase grid-connected converter," *IEEE Trans. Ind. Appl.*, vol. 55, no. 4, pp. 4275–4285, Jul./Aug. 2019.

[78] W. Yao, P. C. Loh, Y. Tang, X. Wang, X. Zhang, and F. Blaabjerg, "A robust DC-split-capacitor power decoupling scheme for single-phase converter," *IEEE Trans. Power Electron.*, vol. 32, no. 11, pp. 8419–8433, Nov. 2017.

[79] Y. Liu, Y. Sun, and M. Su, "Family of two-port switching networks with ripple power decoupling and output voltage step-up functions," *IET Power Electron.,* vol. 10, no. 10, pp. 1175–1182, Aug. 2017.

[80] Y. Liu, Y. Sun, and M. Su, "Active power compensation method for single-phase current source rectifier without extra active switches," *IET Power Electron.,* vol. 9, no. 8, pp. 1719–1726, Jun. 2016.

[81] Y. Sun, Y. Liu, M. Su, X. Li, and J. Yang, "Active power decoupling method for single-phase current-source rectifier with no additional active switches," *IEEE Trans. Power Electron.*, vol. 31, no. 8, pp. 5644–5654, Aug. 2016.

[82] W. Xiong, Y. Liu, Z. Lin, Y. Sun, and M. Su, "Single-phase current source converter with high reliability and high power density," *IET Power Electron.,* vol. 13, no. 6, pp. 1218–1226, May 2020.

[83] C. Xu, M. Zhou, Y. Liu, and Y. Sun, "Transformer-less single-phase unified power quality conditioner of no circulating current," *IET Power Electron.*, vol. 13, no. 5, pp. 970–980, Apr. 2020.

[84] Y. Liu *et al.*, "Single-phase inverter with wide input voltage and power decoupling capability," *IEEE Access*, vol. 7, pp. 16870–16879, 2019.

[85] Y. Liu, Y. Sun, M. Su, M. Zhou, Q. Zhu, and X. Li, "A single-phase PFC rectifier with wide output voltage and low-frequency ripple power decoupling," *IEEE Trans. Power Electron.*, vol. 33, no. 6, pp. 5076–5086, Jun. 2018.

[86] Y. Liu, Y. Sun, M. Su, X. Li, and S. Ning, "A single phase AC/DC/AC converter with unified ripple power decoupling," *IEEE Trans. Power Electron.*, vol. 33, no. 4, pp. 3204–3217, Apr. 2018.

[87] Y. Liu, Y. Sun, M. Su, and F. Liu, "Control method for the Sheppard–Taylor PFC rectifier to reduce capacitance requirements," *IEEE Trans. Power Electron.*, vol. 33, no. 3, pp. 2714–2722, Mar. 2018.

[88] Y. Liu, Y. Sun, and M. Su, "A control method for bridgeless Cuk/Sepic PFC rectifier to achieve power decoupling," *IEEE Trans. Ind. Electron.*, vol. 64, no. 9, pp. 7272–7276, Sep. 2017.

[89] M. Mellincovsky, V. Yuhimenko, Q.-C. Zhong, M. M. Peretz, and A. Kuperman, "Active DC link capacitance reduction in grid-connected power conversion systems by direct voltage regulation," *IEEE Access*, vol. 6, pp. 18163–18173, 2018.

[90] M. Mellincovsky, V. Yuhimenko, M. M. Peretz, and A. Kuperman, "Analysis and control of direct voltage regulated active DC-link capacitance reduction circuit," *IEEE Trans. Power Electron.*, vol. 33, no. 7, pp. 6318–6332, Jul. 2018.

[91] H. Yuan, S. Li, W. Qi, S.-C. Tan, and S.-Y. Hui, "On nonlinear control of single-phase converters with active power decoupling function," *IEEE Trans. Power Electron.*, vol. 34, no. 6, pp. 5903–5915, Jun. 2019.

[92] H. Yuan, S. Li, S.-C. Tan, and S. Y. R. Hui, "Internal dynamics stabilization of single-phase power converters with Lyapunov-based automatic-power-decoupling control," *IEEE Trans. Power Electron.*, vol. 35, no. 2, pp. 2160–2169, Feb. 2020.

[93] M. Mellincovsky, V. Yuhimenko, M. M. Peretz, and A. Kuperman, "Low-frequency DC-link ripple elimination in power converters with reduced capacitance by multiresonant direct voltage regulation," *IEEE Trans. Ind. Electron.*, vol. 64, no. 3, pp. 2015–2023, Mar. 2017.

[94] A. Mutovkin, M. Mellincovsky, V. Yuhimenko, S. Schacham, and A. Kuperman, "Conditions for direct applicability of electronic capacitors to dual-stage grid-connected power conversion systems," *IEEE J. Emerg. Sel. Topics Power Electron.*, vol. 7, no. 3, pp. 1805–1814, Sep. 2019.

[95] W.-L. Ming, Q.-C. Zhong, and X. Zhang, "A single-phase four-switch rectifier with significantly reduced capacitance," *IEEE Trans. Power Electron.*, vol. 31, no. 2, pp. 1618–1632, Feb. 2016.

[96] Q.-C. Zhong and W.-L. Ming, "A θ-converter that reduces common mode currents, output voltage ripples, and total capacitance required," *IEEE Trans. Power Electron.*, vol. 31, no. 12, pp. 8435–8447, Dec. 2016.

[97] A. Mutovkin, V. Yuhimenko, S. Schacham, and A. Kuperman, "Nonlinear control of electronic capacitor for enhanced stability and dynamic response," *IEEE Trans. Ind. Electron.*, vol. 68, no. 8, pp. 6881–6892, Aug. 2021.

[98] G. Yona and G. Weiss, "The virtual infinite capacitor," *Int. J. Control*, vol. 90, no. 1, pp. 78–89, 2017.

[99] S. Li, W. Qi, S.-C. Tan, and S. Y. Hui, "Enhanced automatic-power-decoupling control method for single-phase AC-to-DC converters," *IEEE Trans. Power Electron.*, vol. 33, no. 2, pp. 1816–1828, Feb. 2018.

[100] W. Qi, S. Li, H. Yuan, S.-C. Tan, and S.-Y. Hui, "High-power-density single-phase three-level flying-capacitor buck PFC rectifier," *IEEE Trans. Power Electron.*, vol. 34, no. 11, pp. 10833–10844, Nov. 2019.

[101] S. Hwang, S. Ogasawara, K. Orikawa, and M. Takemoto, "A new active power-decoupling topology and control mechanism to extend the lifespan and reduce the number of passive components," *IEEJ Trans. Elect. Electron. Eng.*, vol. 14, no. 5, pp. 780–791, May 2019.

[102] S. Li, W. Qi, J. Wu, S.-C. Tan, and S.-Y. Hui, "Minimum active switch requirements for single-phase PFC rectifiers without electrolytic capacitors," *IEEE Trans. Power Electron.*, vol. 34, no. 6, pp. 5524–5536, Jun. 2019.

[103] W. Qi, S. Li, S.-C. Tan, and S. Y. Hui, "Design considerations for voltage sensorless control of a PFC single-phase rectifier without electrolytic capacitors," *IEEE Trans. Ind. Electron.*, vol. 67, no. 3, pp. 1878–1889, Mar. 2020.

[104] L. Zhang and X. Ruan, "Control schemes for reducing second harmonic current in two-stage single-phase converter: An overview from DC-bus port-impedance characteristics," *IEEE Trans. Power Electron.*, vol. 34, no. 10, pp. 10341–10358, Oct. 2019.

[105] S. Li, A. T. L. Lee, S.-C. Tan, and S. Y. R. Hui, "Plug-and-play voltage ripple mitigator for DC links in hybrid AC-DC power grids with local bus-voltage control," *IEEE Trans. Ind. Electron.*, vol. 65, no. 1, pp. 687–698, Jan. 2018.

[106] J. Lin and G. Weiss, "Plug-and-play control of the virtual infinite capacitor," *IEEE Trans. Power Electron.*, vol. 35, no. 2, pp. 1947–1956, Feb. 2020.

[107] M. S. Irfan, A. Ahmed, J.-H. Park, and C. Seo, "Current-sensorless power-decoupling phase-shift dual-half-bridge converter for DC–AC power conversion systems without electrolytic capacitor," *IEEE Trans. Power Electron.*, vol. 32, no. 5, pp. 3610–3622, May 2017.

[108] H. Sun, H. Wang, and W. Qi, "Automatic power decoupling controller of dependent power decoupling circuit for enhanced transient performance," *IEEE Trans. Ind. Electron.*, vol. 66, no. 3, pp. 1820–1831, Mar. 2019.

[109] S. Nonaka and Y. Neba, "Single-phase PWM current source converter with double-frequency parallel resonance circuit for DC smoothing," in *Proc. Conf. Rec. IEEE Ind. Appl. Conf. 28th IAS Annu. Meeting*, 1993, pp. 1144–1151.

[110] K. Fukushima, I. Norigoe, M. Shoyama, T. Ninomiya, Y. Harada, and K. Tsukakoshi, "Input current-ripple consideration for the pulse-link DC-AC converter for fuel cells by small series LC circuit," in *Proc. 24th Annu. IEEE Appl. Power Electron. Conf. Expo.*, Washington, DC, USA, 2009, pp. 447–451.

[111] K.-I. Hwu, W.-C. Tu, and C.-Y. Lai, "Light-emitting diode driver with low-frequency ripple suppressed and dimming efficiency improved," *IET Power Electron.*, vol. 7, no. 1, pp. 105–113, Jan. 2014.

[112] S. Li, W. Qi, S.-C. Tan, S. Y. Hui, and C. K. Tse, "A general approach to programmable and reconfigurable emulation of power impedances," *IEEE Trans. Power Electron.*, vol. 33, no. 1, pp. 259–271, Jan. 2018.

[113] J. Lin and G. Weiss, "An indirect approach to control an active capacitor," *IEEE J. Emerg. Sel. Topics Power Electron.*, vol. 8, no. 3, pp. 2898–2906, Sep. 2020.

[114] A. Mutovkin, V. Yuhimenko, M. Mellincovsky, S. Schacham, and A. Kuperman, "Control of direct voltage regulated active DC-link capacitance reduction circuits to allow plug-and-play operation," *IEEE Trans. Ind. Electron.*, vol. 66, no. 8, pp. 6527–6537, Aug. 2019.

[115] Y. Liu, W. Zhang, J. Lin, M. Su, and X. Liang, "Active power decoupling control for single-phase current source rectifier based on emulating LC resonator," *IEEE Trans. Ind. Electron.*, vol. 68, no. 6, pp. 5460–5465, Jun. 2021.

Yonglu Liu (Member, IEEE) was born in Chongqing, China, in 1989. He received the B.S., M.S., and Ph.D. degrees in electrical engineering from Central South University, Changsha, China, in 2012, 2015, and 2017, respectively.

He is currently an Associate Professor with the School of Automation, Central South University. His research interests include power electronics and renewable energy power conversion systems.

Wanlu Zhang was born in Fujian, China, in 1997. She received the B.S. degree in electrical engineering in 2019 from Central South University, Changsha, China, where she is currently working toward the M.S. degree in electrical engineering.

Her current research interests include modeling and control of power electronics' devices.

Yao Sun (Member, IEEE) was born in Hunan, China, in 1981. He received the B.S., M.S., and Ph.D. degrees from Central South University, Changsha, China, in 2004, 2007, and 2010, respectively.

He has been a Professor with the School of Automation, Central South University. His research interests include matrix converter, microgrid, and wind energy conversion system.

Mei Su (Member, IEEE) was born in Hunan, China, in 1967. She received the B.S., M.S., and Ph.D. degrees from the School of Information Science and Engineering, Central South University, Changsha, China, in 1989, 1992, and 2005, respectively.

She has been a Full Professor with the School of Automation, Central South University. She is currently an Associate Editor for the IEEE TRANSACTIONS ON POWER ELECTRONICS. Her research interests include matrix converter, adjustable speed drives, and wind energy conversion system.

Guo Xu (Member, IEEE) received the B.S. degree in electrical engineering and automation and the Ph.D. degree from the Beijing Institute of Technology, Beijing, China, in 2012 and 2018, respectively.

From 2016 to 2017, he was a Visiting Student with the Center for Power Electronics System, Virginia Polytechnic Institute and State University, Blacksburg, VA, USA. Since 2018, he has been with the School of Automation, Central South University, Changsha, China, where he is currently an Associate Professor. His research interests include modeling and control of power electronics converters, high-efficiency power conversion, and magnetic integration in power converters.

Hanbing Dan (Member, IEEE) was born in Hubei, China, in 1991. He received the B.S. degree in automation and the Ph.D. degree in control science and engineering from Central South University, Changsha, China, in 2012 and 2017, respectively.

He was a Visiting Researcher with the Faculty of Engineering, University of Nottingham, U.K., in 2017. He is currently an Associate Professor with the School of Automation, Central South University. His research interests include power converter, motor control, model predictive control, and fault diagnosis.